A
Dissertation
on

MODELLING AND SIMULATION OF HOT-WALL CONDENSER

Submitted in partial fulfillment of the requirement for the award of Degree of

MASTER OF ENGINEERING
(Thermal Engineering)

Submitted by
NITIN JAIN
(University Roll No. 2201)

Under the Guidance of
Prof. A. K. PRATIHAR

DEPARTMENT OF MECHANICAL ENGINEERING
DELHI COLLEGE OF ENGINEERING
BAWANA ROAD, NEW DELHI
(DELHI UNIVERSITY)

JUNE-2007

CERTIFICATE

This is to certify that the M.E. Major project entitled **"Modelling and Simulation of Hot-Wall Condenser"** submitted by Mr. Nitin Jain, Department of Mechanical Engineering, Delhi College of Engineering, Delhi University, Delhi, embodies the original work carried out by him under my supervision and guidance. His work has been found excellent for the partial fulfillment of the requirement of the degree of M.E. in Thermal Engineering.

The project has been carried out during the session 2006-2007.

To the best of my knowledge and belief, this work has not been submitted to any other University or Institute for the award of any degree or diploma.

(A. K. Pratihar)
Assistant Professor
Department of Mechanical Engineering
Delhi College of Engineering
Bawana Road, Delhi-42

ABSTRACT

Heat exchangers play an important role in a variety of energy conversion applications. They have a significant impact on the energy efficiency, cost, size, and weight of energy conversion systems.

This project report presents modelling and simulation results of hot-wall condensers that are commonly used in vapour compression cycle based domestic refrigerators. A simulation model is developed to analyse the heat transfer and pressure drop characteristics of the condenser. The model is based on variable conductance approach, and is developed using a combination of thermodynamic correlations. The simulation is carried out using Engineering Equation Solver (EES).

The parameters computed in this study, are inner heat transfer coefficient (refrigerant side) and outer heat transfer coefficients (air side), condenser capacity and pressure drop. The simulation is done for whole length of condenser tube, and the effects of operating parameters such as mass flow rate and ambient temperature are also studied. The simulation results are validated by comparing the results with those reported by other investigators. The aim of this project is also to compare the performance of hot-wall condenser due to use of R134a refrigerant in place of R12.

In this work, it has been found that the performance of condenser with R134a refrigerant is marginally lower than that of with R12. The pressure drop for R134a has also been found to be about 10 % higher as compared to that obtained with R12. However, it is well known that R134a refrigerant is an ozone friendly refrigerant which is a suitable replacement of R12.

ACKNOWLEDGEMENT

It is distinct pleasure to express my deep sense of gratitude and indebtedness to my guide Prof. A.K.Pratihar, Department of Mechanical Engineering, Delhi College of Engineering, for his invaluable guidance, encouragement and patient review. His continuous inspiration has made me complete this dissertation successfully.

I would also like to take this opportunity to present my sincere regards to my teachers for their kind support and encouragement. I am grateful to my parents, brothers and sisters for their moral support all the time; they have been always around on the phone to cheer me up in the odd times of this work.

I am also thankful to my friends and classmates for their unconditional support and motivation for this major report.

I am also thankful to all other persons who helped me throughout the course of this dissertation.

(NITIN JAIN)
M.E. (Thermal Engineering)
Department of Mechanical Engineering
Delhi College of Engineering
Bawana Road, Delhi-42

TABLE OF CONTENTS

LIST OF FIGURES

LIST OF TABLES

NOMENCLATURE

A	area (m^2)
d	diameter (m)
E_h	enthalpy (J /kg)
f	friction factor (–)
g	acceleration due to gravity (m/ s^2)
G	Mass flux (kg /m^2- s)
h	heat transfer coefficient (kg/m^2-K)
h_{fg}	heat of vaporisation (J /Kg)
k	thermal conductivity (W/m- K)
L	length (m)
m	fin property parameter (–)
$\dot{m}$	mass flow rate (kg/ s)
Nu	Nusselt number (–)
P	Pressure (kPa)
Pr	Prandtl number (–)
Q	heat flow rate (W)
q	heat flux (W/m^2)
R	thermal resistance (K /W)
Ra	Rayleigh number (–)
Re	Reynolds number (–)
T	temperature (K)
U	unit conductance (W/m^2-K)
w_{av}	average width (m)
x	refrigerant quality (–)
X_{tt}	Martinelli parameter (–)
Δz	elemental length (m)

GREEK LETTERS

Π pie (–)

β thermal expansion coefficient (1/K)

ε thermal emittance (–)

η efficiency (–)

υ kinematic viscosity (m2 /s)

ρ density (kg m3)

σ Stefan–Boltzmann constant

SUBSCRIPTS

a air/accelerational

c convective

c and r convection and radiation

conduct conduction

cha characteristic

ele elemental

eq equivalent

f frictional

g gravitational

i inside, inlet

l liquid phase

o outside, outlet

pl plate

r radiative

ref refrigerant

t tube

tot total

v vapor/gas phase

∞ free stream/ambient

Chapter 1

INTRODUCTION

As electric-generating capacity grew and as homes were beginning to be wired for its use, household refrigerators became more popular and began replacing the common window and standing iceboxes. The interest and demand for household refrigerators was aided by the design and development of fractional horsepower motors, which were used in refrigerators. These units began being produced in large numbers in the early 1920s and have become a necessity for all.

Currently, refrigeration research focuses on improving energy efficiency, reducing manufacturing cost and introducing innovative designs of heat exchangers (compact, functional, user-friendly). A well-designed condenser will not only improve the energy efficiency, but will also reduce the space and material for a specific cooling capacity.

The refrigerant-to-air condenser for condensing the refrigerant forms an important component of any refrigeration cycle. One reason for this is that the overall effectiveness of the cycle is influenced by the effectiveness of condenser. It is desirable to keep the temperature difference, ΔT, between the refrigerant and the air in the condenser as small as possible. This leads to lowering in the ΔT over which heat must be transferred and thus to an increase in the coefficient of performance (COP).

A domestic refrigerator uses an air cooled condenser as a heat exchanger to reject heat to the surroundings. In earlier designs of domestic refrigerators, wire and tube condensers were used. In such types of condensers, tubes are exposed to atmosphere, hence they are likely to be damaged during handling. Also due to deposition of dirt, the outside heat transfer coefficient decreases significantly and thus their performance adversely affected. In most of the recent designs hot-wall condensers become popular due to above mentioned weaknesses of wire and tube condenser. It is therefore desirable to investigate the performance of this type of condenser under various operating conditions.

In order to develop a high quality cycle simulation for vapor compression systems it is essential to have an accurate condenser model. In such situation computer simulation would act as a convenient tool for analysing the performance of the condenser for different operating parameters such as ambient temperature, mass flow rate etc., and reducing the cost of prototype testing of new condensers.

This work presents the simulation results for hot-wall condenser of a domestic refrigerator under various operating condition for two refrigerants viz., R134a and R12.

Refrigerant R12 was earlier used in domestic refrigerators which is now banned because it depletes ozone layer. R134a is being used now a days to replace R12 because the former has zero depleting potential. This work also aims to study the deviation in the performance of condenser due to replacement of R12 by R134a.

Chapter 2

LITERATURE REVIEW

As the discussing is going on about simulation of condensers in domestic refrigerator, it is important to know about some basics and previous work in this field. These are:

2.1 Types of Condensers for Domestic Refrigerator: Two most commonly used design of condensers used in domestic refrigerators are:

1 Wire and tube condenser

2 Hot-wall condenser

2.1.1 Wire and tube condenser

One of the commonly used condensers in domestic refrigerators is the wire-and-tube condenser. As described by Tagliafico and Tanda [1997], the wire-and-tube condenser is predominantly a natural convection heat exchanger. It consists of a single copper tube and solid steel wires that serve as extended surfaces. The tube which carries the refrigerant is bent into a single-passage serpentine shape with wires symmetrically spot-welded to both sides in a direction normal to the tube as shown in Fig. 2.1. It had been used and widely studied since 1960s. In this type of condenser the major heat transfer at outer side of the tube is due to convection.

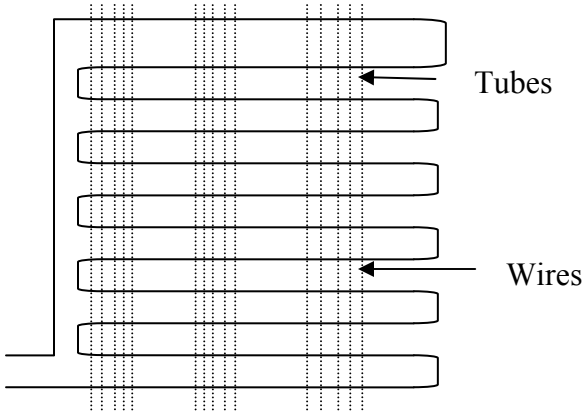

Fig.2.1 Schematic diagram of wire and tube condenser

A conventional refrigerator uses a wire-and-tube condenser, which is attached to the back of the refrigerator. However, this condenser is prone to be damaged and dirt tends to accumulate and form a scale layer on the hot surface. This increases the fouling resistance and reduces the heat transfer significantly from the condenser. Due to these factors, a new condenser design, called the ‘‘hot-wall condenser’’ was introduced in recent years to replace the wire-and tube condenser

2.1.2 Hot-wall condenser

The hot-wall condenser, also known as wrapper type condenser, consists of steel tubing (coated with copper), which is installed by direct contact on the inner surface of the outer steel plate of side walls of a refrigerator as shown in Fig. 2.2. As described by Bansal and Chin [2002], the adhesive aluminium foil holds the tube in place and acts as a shield to prevent heat transfer into the refrigerating compartment. Since the condenser tubing is installed in a refrigerator wall, which is usually hot, it is called ‘‘hot-wall condenser’’. There are four panels namely the left, right, back and base panel, each with distinct tube configurations as shown in Fig.2.2b. The refrigerant flows from the back panel to the base panel, then to the right-hand side panel and through the cross rail to the left-hand side panel. In this type of condenser the major heat transfer at outer side of the tube is due to radiation.

2.1.3 Justification for choosing hot-wall condenser

The heat path of a hot-wall condenser is rather complicated. After heat transfer from the condensing refrigerant to the tube wall, the heat is conducted through the aluminium foil to the plate as well as the foam insulation. Generally, the major amount of heat will be dissipated to the surroundings through the outer plate by means of convection and radiation, while small amount will end up infiltrating into the refrigeration compartment. This condenser is a relatively new design. The lack of published studies on the hot-wall condenser is probably a consequence of this factor as well as the non-uniformity between each design and the complex heat path. No study could be found in the literature either on experimental or the theoretical aspects of the hot wall condenser. Therefore, this

investigation is unique and aims to characterise the heat transfer performance of the condenser.

It is envisaged that a computer model would act as a convenience tool for analysing the performance of the condenser for different design parameters such as ambient temperature and mass flow rate, and reducing the cost of prototype testing of new condensers.

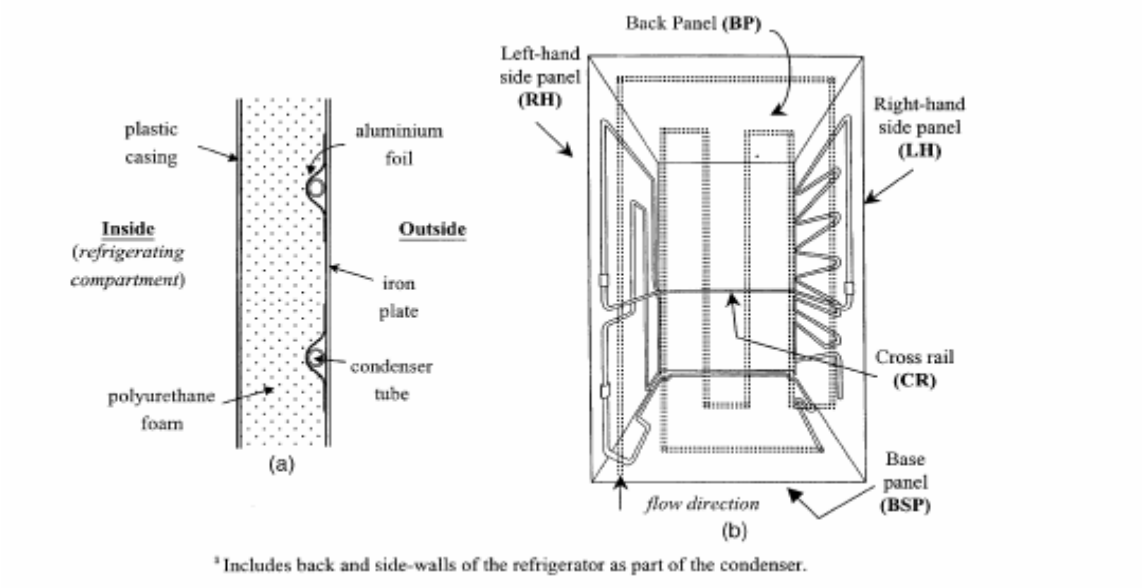

Fig.2.2 Hot-wall condenser (a) cross section of a hot-wall condenser on refrigerator's wall, (b) configuration and setup of tubing for a hot-wall condenser.[Bansal and Chin [2002]]

2.2 Condensation

Condensation in hot-wall condenser will take place when vapour flows by forced convection over a surface maintained at a temperature lower than the saturation temperature of the fluid. Condensation under these conditions is called forced convection condensation. Heat transfer rates in forced convection condensation are substantially higher than those of pool condensation. Depending on the wetting properties of the cooled surface, the condensate will either wet the surface or spread out to form a continuous film or discrete droplets.

2.2.1 Modes of condensation

There are two different modes of condensation. They are following as:

2.2.1.1 Film condensation

If the liquid wets the surface, a smooth film is formed and the process is called film condensation. The latent heat released on condensation is conduct through this film from the interface where the condensation occurs and is removed through the tube wall.

2.2.1.2 Drop wise condensation

If the liquid does not wet the surface, droplets are formed which is called drop wise condensation. The drops therefore do not form a continuous film; instead it reaches a critical size and run down the surface. The surface is left dry and another drop can begin to form. The condensing coefficient is significantly larger than film wise condensation because the vapour is in direct contact with the wall. Because, drop wise condensation is difficult to promote reliably, the normal design practice in engineering such as refrigeration, steam power and dehumidification plants is based on the assumption of film condensation.

2.2.2 Flow models

The effective design and operation of these and similar systems depend to a large extend on the mechanism of heat transfer across the free surface of the liquid and the hydrodynamic conditions at the free surface of the liquid film. Unfortunately these phenomena are quite complicated and not amenable to a simple analytical treatment. Empirical or semi-empirical models were developed and are based on either homogeneous flow or separate flow assumptions.

2.2.2.1 Homogeneous flow model

The homogeneous flow model assumes that the two phases are well mixed and travel with equal velocities. In this model the physical properties of the two phases are defined as a mean value of the liquid and gas phase respective properties.

2.2.2.2 Separate flow model

In the separate flow model the phases flow with separate different velocities, with separate different properties. The ratio of the vapour/liquid velocity is called the slip ratio. For separate flow it is thus greater than unity. The separate flow model is most sufficient in annular flow when the liquid attach itself as a thin film along the circumference of the tube while the vapour core flows in the central region. For high vapour velocities, the vapour core has a higher velocity than the liquid film with separate properties.

2.2.3 Flow patterns

Condensation inside tubes is of considerable practical interest because of applications to condensers in refrigeration and air-conditioning systems. As the quality of the vapour changes, the flow conditions or a pattern changes as well. In gas-liquid flow the two phases can adopt various geometric configurations known as flow patterns or regimes. Many research papers have defined several flow patterns; many of these are merely alternative names. The most sensibly defined regions are as told by Whalley [1987]: stratified, wavy, slug, churn, annular, bubbly and mist flow.

1. **Laminar or Stratified flow**

   In this type of flow both phases flowing beside each other are separated by a plane surface. This occurs when the liquid vapour interface is smooth, which is highly uncommon in practice.

2. **Wavy flow**

   In this type of flow both phases are separated by a wavy surface. This is more common in practice than stratified.

3. **Slug flow**

   In this flow slugs of the liquid are enclosed in the gas stream. Slug flow occurs when the amplitude is so large that the wave touches the top of the tube.

4. Annular flow

During annular flow the liquid travels partly as an annular film on the walls of the tube and partly as small drops distributed in the gas, which flow in the center of the tube. The occurrence of this phase of condensation can be expected when the mixture velocity exceeds 2 m/s.

5. Bubbly flow

In bubbly flow the vapour bubbles are of uniform size and tend to flow along the top of the tube.

6. Churn or plug flow

A highly unstable flow of an oscillatory nature is called churn flow.

7. Mist or foam flow

This flow occurs with the flow patterns corresponding to definite mass flow rates or liquid velocities.

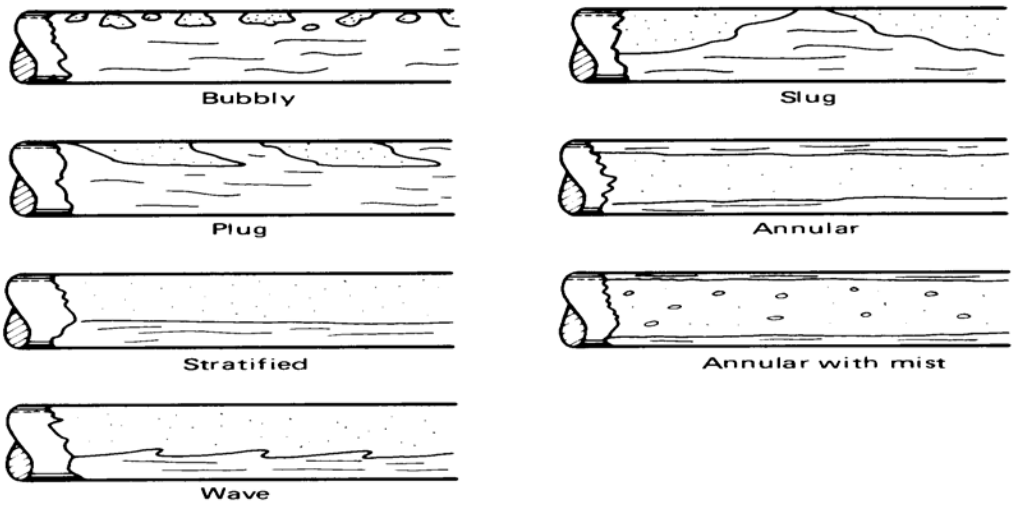

Fig.2.3 Different types of flow pattern in two phase flow

2.3 Previous Work

As very little work has done in this field so far. Yet there are some men who did a great work in this field. There work can be described as:

1. Radermacher and Kim [1996] took the first step in this area. They gave the information regarding the demerits of conventional refrigerator in his research paper named as "*Domestic refrigerators: recent developments*". This paper summarizes recent developments in the field of domestic household refrigerators based on a survey of publications and patents.

2. Bansal and Chin [2002] developed a simulation model for the hot-wall condenser for the refrigerant R134a in FORTRAN90 language. They gave all results in their paper named as *"Design and modelling of hot-wall condensers in domestic refrigerators"*. This paper presents the experimental and modelling results of hot-wall condensers that are commonly used in domestic vapour compression based refrigerators. Experiments were carried out on a real refrigerator using R134a as the refrigerant to obtain the condenser capacity, pressure loss and degree of subcooling at different operating conditions. A simulation model was developed to analyse the heat transfer characteristics of the condenser.

3. Bansal and Chin [2003] did the modelling and optimization of wire and tube condenser in the FORTRAN90 language. They optimized condenser capacity and gave all results in his research paper named as "*Modelling and optimisation of wire-and-tube condenser"*. This paper presents the modelling and experimental results of wire-and-tube condensers that are commonly used in vapour compression cycle based domestic refrigerators. The condenser capacity per unit weight was optimised using a variety of wire and tube pitches and diameters. An optimisation factor, f_o was defined as ratio of the condenser capacity per unit weight of the optimised design and the present design.

4. Rousseau, Eldik and Greyvenstein [2003] did the detailed simulation for fluted tube type condenser. They gave the results for both static and transient conditions. They gave

all results in their combined research paper named as *"Detailed simulation of fluted tube water heating condensers*". This paper describes the development of a detailed model to simulate fluted tube refrigerant-to-water condensers. The model allows the surface area to be divided into any number of sections for which all the refrigerant and water properties can be evaluated. This allows for the extension of the model to simulate heat exchangers for cycles employing zeotropic refrigerant mixtures.

2.4 About this Project

In this project, modelling and simulation of hot-wall condenser has been done. Modelling is based on various thermodynamic correlations and the simulation program is written in the EES language. The simulation is carried out for two refrigerants i.e. R134a and R12 which are used in domestic refrigerator.

Comparison between the two is also carried out in this project so that the deviation in performance of the condenser, due to use of R134a in place of R12, can be shown.

The parameters which are calculated in the simulation are outer and inner side heat transfer coefficients, overall heat transfer coefficient, heat flow rate in the tubes and pressure drop. Later the effect of parameters like ambient temperature and mass flow rate on various heat transfer coefficients viz. refrigerant side, outside radiative and convective heat transfer coefficients, condenser heat load (heat rejected) is also studied.

As in vapour compression cycle, refrigerant in the condenser comes directly from compressor in superheated state, the length of tube used for desuperheating is also calculated. The simulation is started from the saturated vapour state. Therefore it is also important to know about desuperheating length of tube, in which refrigerant state changes to saturated vapour from superheated vapour state.

For validation, the results for R134a have been compared with the results published in the literature.

2.5 Engineering Equation Solver [1992-2006]

EES (pronounced 'ease') is an acronym for Engineering Equation Solver. The basic function provided by EES is the solution of a set of algebraic equations. EES can also solve differential equations, equations with complex variables, do optimization, provide linear and non-linear regression, generate publication-quality plots, simplify uncertainty analyses and provide animations. EES has been developed to run under 32-bit Microsoft Windows operating systems, i.e., Windows 95/98/2000/XP.

There are two major differences between EES and existing numerical equation-solving programs. First, EES automatically identifies and groups equations that must be solved simultaneously. Second, EES provides many built-in mathematical and thermophysical property functions useful for engineering calculations. For example, the steam tables are implemented such that any thermodynamic property can be obtained from a built-in function call in terms of any two other properties. Similar capability is provided for most organic refrigerants (including some of the new blends), ammonia, methane, carbon dioxide and many other fluids. Air tables are built-in, as are psychrometric functions and data for many common gases. Transport properties are also provided for most of these substances.

EES allows the user to enter his or her own functional relationships in three ways. First, a facility for entering and interpolating tabular data is provided so that tabular data can be directly used in the solution of the equation set. Second, the EES language supports user-written Functions and Procedures similar to those in Pascal and FORTRAN. EES also provides support for user-written routines, which are self-contained EES programs that can be accessed by other EES programs. The Functions, Procedures, Subprograms and Modules can be saved as library files which are automatically read in when EES is started. Third, external functions and procedures, written in a high-level language such as Pascal, C or FORTRAN, can be dynamically-linked into EES using the dynamic link library capability incorporated into the Windows operating system. These three methods of adding functional relationships provide very powerful means of extending the capabilities of EES.

Chapter 3

MODELLING AND SIMULATION

Modelling and simulation of hot-wall air cooled condenser has been discussed in this chapter.

3.1 Model for the Hot-Wall Condenser

A simulation model is developed for the hot-wall condenser using the variable conductance approach, along with a combination of thermodynamic correlations. It is written in EES (Engineering Equation Solver) programming language.

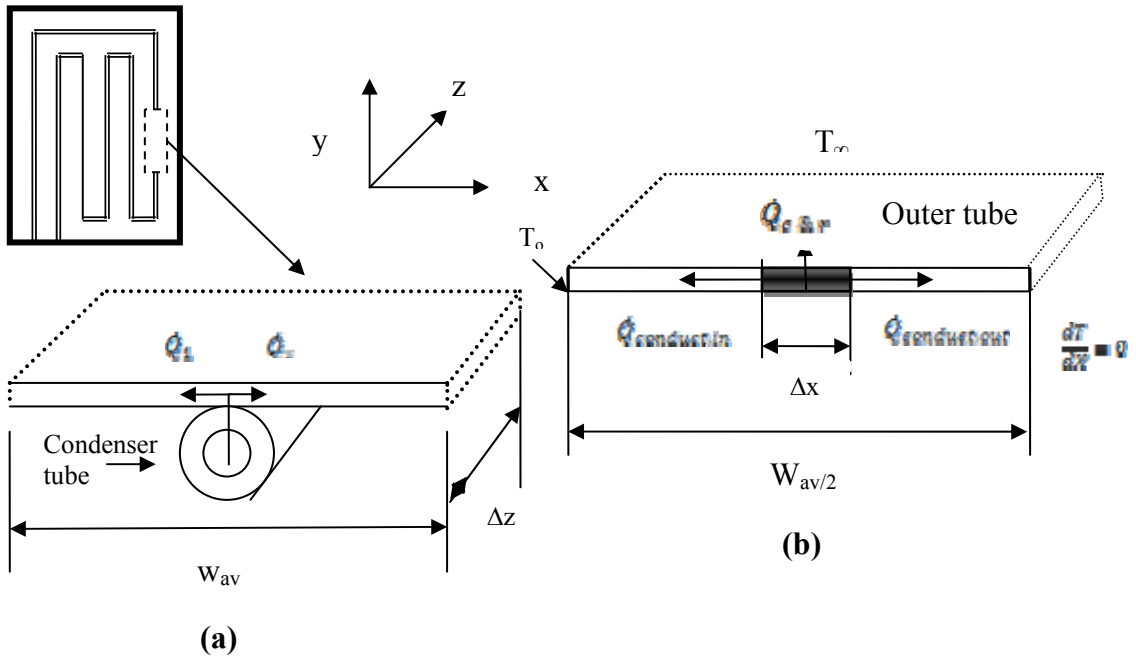

Fig.3.1 (a) Cross sectional view of an element of the hot-wall condenser tubing and direction of heat flow. (b) Heat transfer mechanism and boundary conditions along the outer plate.

The hot-wall condenser is divided into various panels and all individual panels are behaving as elemental units. Each element of the condenser is made up of a tube-and-plate configuration with an elemental length of Δz as shown in Fig.3.1(a). Since a small

amount of heat conducts through the aluminium foil to the foam insulation, it has been neglected in the condenser modelling. Fig.3.2 shows the cross section of an element extracted from a specific panel of the fridge (left, right or back as shown in Fig. 2.2) where the refrigerant flows in the z-direction. To simplify the analysis as did by Bansal and Chin [2002], an average width, w_{av} for each panel is computed as follows:

$$w_{av} = \frac{\text{Total area of the specific panel}}{\text{Total tube length on the specific panel}} \tag{3.1}$$

The outer heat transfer area of the plate corresponding to an element, A_{pl} is given by:

$$A_{pl} = w_{av}\Delta z \tag{3.2}$$

Now to find the elemental heat transfer, variable conductance approach is applied to each element. The rate of heat transfer from an element of length Δz as shown in fig.3.1 is given by:

$$\dot{Q}_{ele} = UA_{ele}(T_{ref} - T_{\infty})_{ele} \tag{3.3}$$

Where the variable conductance, UA_{ele} for each element can be calculated as:

$$\frac{1}{UA_{ele}} = R_{tot.ele} = R_i + R_t + R_{con} + R_{o,eq} \tag{3.4}$$

As shown in Eqn (3.4) it is a function of the inner (R_i), tube (R_t), contact (R_{con}) and outer heat transfer resistances ($R_{o,eq}$). The first three components of the resistances can be found from conventional heat transfer equations while the fourth component, $R_{o,eq}$ has to be derived. Generally, heat is conducted along the plate while simultaneously being convected and radiated from the plate upper surface. $R_{o,eq}$ represents the resistance

against the heat transfer from the contact point, through the plate to the surrounding. The quantification of this outer heat transfer resistance is realised in the following steps.

3.1.1 One-dimensional heat transfer in the plate

The temperature is assumed to be virtually constant across the whole element in z-direction. This is particularly true when the refrigerant undergoes constant temperature condensation process. In the superheated or sub-cooled region, the estimated temperature difference across element is only 0.05 °C and therefore, the effect of temperature gradient is negligible. Regarding the temperature distribution of the plate in the y-direction, it is virtually constant because the plate is very thin. Therefore, as the temperature is constant in the y- and z-directions, the heat flow can be assumed to be one-dimensional within the plate in the x-direction.

3.1.2 Computation of outer heat transfer coefficient

The outer heat transfer coefficient is the summation of the radiative and convective heat transfer coefficient as:

$$h_0 = h_c + h_r \tag{3.5}$$

To find the convective and radiative heat transfer coefficients, the average temperature of the plate, $T_{pl,av}$ is to be computed. $T_{pl,av}$ is determined by the tube temperature (outer surface,T_0), ambient temperature(T_∞), and plate efficiency (η_{pl}) given by:

$$T_{pl.av} = \eta_{pl}(T_0 - T_\infty) + T_\infty \tag{3.6}$$

Where T_0 is the temperature of the plate at x =0 position and is initially guessed at a temperature which is 0.5 °C lower than the refrigerant temperature, $T_{ref.}$ The plate efficiency is given by:

$$\eta_{pl} = \frac{\left[\tanh\left(\frac{mw_{av}}{2}\right)\right]}{\frac{mw_{av}}{2}} \tag{3.7}$$

Where

$$m = \sqrt{\frac{h_o \Delta z}{k_f A_c}} \tag{3.8}$$

Initially, the value for the outer heat transfer coefficient, h_0 is guessed. The convective heat transfer heat transfer coefficient on outer side of plate has been computed using the experimental correlation of the averaged Nusselt number for isothermal vertical flat plate is given by following equation as given by Kothadaraman and Subramanyam [2004]:

$$\overline{Nu} = 0.68 + 0.67\left[Ra_L^{0.25}\left[1+\left(\frac{0.492}{Pr}\right)^{9/16}\right]^{-4/9}\right] \tag{3.9}$$

Where Ra is the Rayleigh number and Pr is the Prandlt number. And Rayleigh number can be calculated as:

$$Ra = \frac{g\beta\,(\,T_{pl,av} - T_\infty\,)L_{cha}^3}{\nu_\infty \alpha} \tag{3.10}$$

Eqn (3.9) is valid for both laminar and turbulent flow. Bansal and Chin [2002] have used separate correlations for laminar and turbulent flow. The characteristic length, L_{cha} for a vertical flat surface is taken equal to the height of the plate. The convective heat transfer coefficient is related to the Nusselt number as:

$$h_c = \frac{\overline{Nu}\, k_a}{L_{cha}} \tag{3.11}$$

The radiative heat transfer coefficient is related to the average plate temperature as below:

$$h_r = \varepsilon\sigma \frac{(T_{pl,av}^4 - T_\infty^4)}{(T_{pl,av} - T_\infty)} \tag{3.12}$$

The summation of the h_c and h_r is compared against the initial guessed value of h_o used in Eqn (3.8). The iterative process is repeated until h_o converges. This is the outer heat transfer coefficient iteration loop, which is labeled as ‘‘h_o loop’’ in the flowchart in Fig. 3.2.

3.1.3 Computation for the elemental heat transfer

Considering a section of the plate as shown in Fig. 3.1, heat is transferred by conduction through the plate in x-direction as well as by convection and radiation through the upper surface to the ambient. An energy balance of the incremental section of length Δx yields

$$\dot{Q}_{conduct,in} + \dot{Q}_{c\ and\ r} = \dot{Q}_{conduct,out} \tag{3.13}$$

or in the differential form as given by Incropera and Witt [1990]

$$\frac{d^2T}{dx^2} - \frac{h\Delta z}{k_{pl}A_c} (T - T_\infty) = 0 \tag{3.14}$$

Where boundary conditions are:

$$x = 0,\ T = T_o \ \text{ and } x = L = \frac{w_{av}}{2},\ \frac{dT}{dx} = 0 \tag{3.15}$$

The second boundary condition, in physical term, means that the temperature gradient is zero at the mid span of the plate between adjacent tubes. This means that there was no heat transfer across the mid span boundary. Thus, the validity of the second boundary condition would suggest that modelling the hot-wall condenser, as a separate unit of tube-plate configuration with a heat transfer constraint at the ‘‘imaginary edge’’ is valid. Now, considering only the area of plate to the right of the tube, the rate of heat transfer from that side of the plate to the surrounding is given as:

$$\dot{Q}_1 = \sqrt{h_o \Delta z k_{pl} A_c}\ (\ T_0 - T_\infty\ )\ \tanh\ (mL) \tag{3.16}$$

3.1.4 Computation of equivalent outer heat transfer using parallel heat flow mechanism

The heat resistance of one side of the plate can be given as

$$R_{pl} = \frac{1}{\sqrt{h_o \Delta z k_{pl} A_c}\tanh\ (\ mL\ )} \tag{3.17}$$

If we consider the heat flow mechanism (Fig.3.1 a), the heat will flow from the tube to the center of the plate and parallel to both sides of the plate. It is assumed that heat is transferred equally to both sides of the plate, that is, $Q_1 = Q_2$. Thus, we can have an equivalent resistance for the parallel heat flow, which can be applied to the whole plate surface as:

$$R_{o,eq} = \frac{R_{pl,1} R_{pl,2}}{R_{pl,1} + R_{pl,2}} = \frac{R_{pl}^2}{2R_{pl}} = \frac{R_{pl}}{2} \quad \text{since } R_{pl,1} = R_{pl,2} = R_{pl} \tag{3.18}$$

Like this the outer equivalent heat transfer resistances can be compute. By applying conventional correlations for other components of the heat resistances, Eqn (3.4) can be rewritten as:

$$R_{tot,ele} = \left(\frac{1}{h_i A_i} + \frac{\ln\left(\frac{r_o}{r_i}\right)}{2\pi k_t \Delta z} + \frac{2\sqrt{h_o \Delta z k_{pl} A_c}\tanh(mL)}{h_o \Delta z k_{pl} A_c \left[\tanh(mL)\right]^2} \right)_{ele} \tag{3.19}$$

Here the contact resistance has been neglected because the contact resistance is negligible as it contributes less than 1% of the total resistance. Next, the inner heat transfer coefficient should be computed. The single-phase heat transfer coefficient is determined using the conventional Dittus–Boelter correlation given by Incropera and Witt [1990]. For condensation inside a tube, a variety of flow patterns can exist. In this study, only two most common flows are considered, namely, the annular and stratified flow, which depend on whether vapor shear or gravitational forces are more important. The flow pattern transitions were predicted according to Breber [1980] method. To compute the condensation heat transfer coefficient for annular flow, Cavillini and Zecchin [1971], correlation is used. It uses an equivalent Reynolds number Re_{eq} to replace the normal Reynolds number used in the most common Nusselt correlations as shown below:

$$Nu_{cond} = \frac{h_i d_{t.i}}{k_l} = 0.5 Re_{eq}^{0.8} Pr_l^{0.33} \tag{3.20}$$

Re_{eq} is computed using the liquid and vapour Reynolds number, Re_l and Re_v given by:

$$Re_{eq} = Re_v \left(\frac{\mu_v}{\mu_l}\right)\left(\frac{\rho_l}{\rho_v}\right)^{0.5} + Re_l \tag{3.21}$$

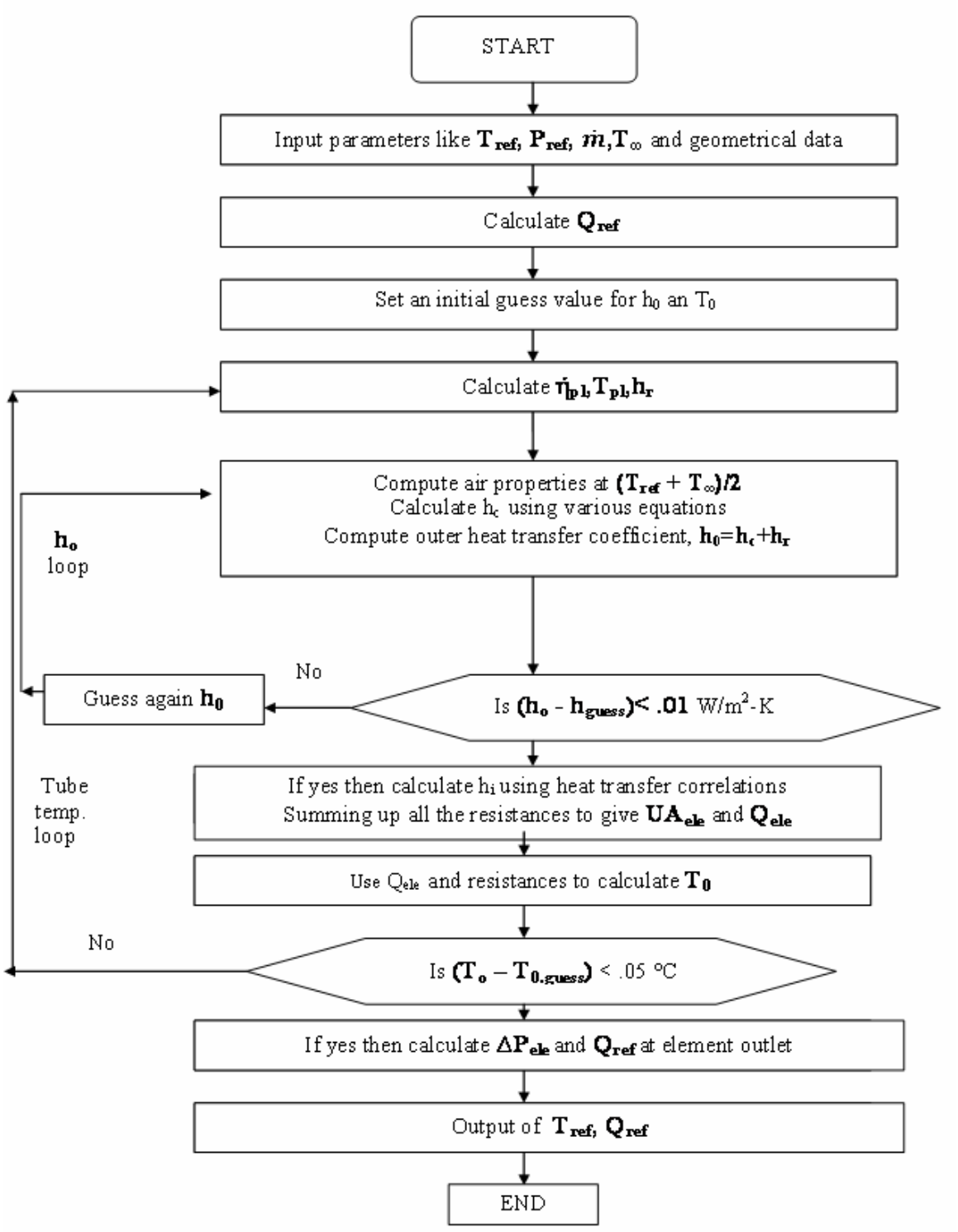

Fig.3.2 Flow chart for the computer model for the condenser

Where

$$Re_l = \frac{G\,(1 - x)\,d_{t,i}}{\mu_l} \text{ And } Re_v = \frac{G\,x\,d_{t,i}}{\mu_v} \tag{3.22}$$

Where G is the mass flux and can be calculated as:

$$G = \frac{\dot{m}}{A_i} \tag{3.23}$$

The average heat transfer coefficient for stratified flow is given by a modified Nusselt number as given by Kakac [1998]:

$$h_m = \Omega \left[\frac{\left(\rho_l\,(\rho_l - \rho_v)\,g h_{fg} k_l^3\right)}{\left(d_{t,i}\mu_l \Delta T\right)} \right]^{0.25} \tag{3.24}$$

Where the coefficient Ω depends on the fraction of the tube that is stratified. Jaster, Kosky [1976] had shown that Ω is related to the void fraction of the vapour, α_g as:

$$\Omega = 0.728\alpha_g^{3/4} \tag{3.25}$$

Where

$$\alpha_g = \frac{1}{1 + \left[(1 - x)/x\right]\left(\frac{\rho_v}{\rho_l}\right)^{2/3}} \tag{3.26}$$

For downward flow of refrigerant in a vertical tube, the following condensation equations can be used depending on the Reynolds numbers as described by Mueller [1983]:

$$\frac{h}{k}\left[\frac{\mu^2}{\rho_l\,(\rho_l - \rho_v)g}\right]^{1/3} = 1.1\mathrm{Re}^{1/3} \quad \text{For } \mathrm{Re} \le 40 \tag{3.27}$$

For Re > 40, the higher of the two coefficients as calculated from the rippled laminar or the turbulent equations as given below, were used.

$$\frac{h}{k}\left[\frac{\mu^2}{\rho_l\,(\rho_l - \rho_v)\,g}\right]^{1/3} = 0.8\mathrm{Re}^{-0.22} \quad \text{For rippled laminar flow} \tag{3.28}$$

$$\frac{h}{k}\left[\frac{\mu^2}{\rho_l\,(\rho_l - \rho_v)\,g}\right]^{1/3} = 0.023\mathrm{Re}^{1/4} \quad \text{For turbulent flow} \tag{3.29}$$

For the upward vapour flow with a returning condensate, the coefficient is given by Mueller [1983] as:

$$\frac{h}{k}\left[\frac{\mu^2}{\rho_l\,(\rho_l - \rho_v)\,g}\right]^{1/3} = 1.47\mathrm{Re}^{-1/3} \tag{3.30}$$

Using the inner and outer heat transfer coefficients, the elemental heat transfer, Q_{ele} is computed from Eqns (3.3), (3.4) and (3.19). As the heat transfer from the refrigerant to the ambient must equal to the heat transfer from the refrigerant to the tube outer surface, the heat transfer can be written as:

$$T_o = T_{ref} - \dot{Q}_{ele}\left(\frac{1}{h_i A_i} + \frac{\ln\left(\frac{r_o}{r_i}\right)}{2\pi k_t \Delta z}\right) \tag{3.31}$$

Therefore, the tube outer temperature $T_{t,o}$ is obtained. This value is then compared against the initial value of T_o. If the error is larger than 0.05 °C, a new T_o is substituted in the Eqn (3.6) and the computations are repeated until convergence is achieved. So that the actual heat rejected can be computed. This iteration loop is called 'tube temperature loop' as shown in Fig.3.2. The enthalpy of the refrigerant at the outlet of an element is:

$$E_{h_o,ele} = \frac{\dot{Q}_{ele}}{\dot{m}} + E_{h_i,ele} \tag{3.32}$$

3.1.5 Pressure drop correlations

The total pressures changes across the condenser, is the summation of the frictional, accelerational and gravitational loss. For single-phase flow, the friction loss is given by Mills [1999] as:

$$\frac{dp}{dz} = -f \frac{1}{d_{t.i}} \frac{\dot{m}^2}{2\rho} \tag{3.33}$$

Where

$$f = (0.79\ln (Re_d) - 1.64)^{-2} \tag{3.34}$$

The two-phase frictional pressure drop generally constitutes the largest part of total pressure drop, although its calculation can only rely extensively upon empirical methods. It involves not only the transfer of momentum or shear stress between the fluid and the wall, but also the transfer of momentum between the individual phases. For the calculation of the frictional pressure drop, it is advantageous to define several parameters that are suitable for the description of the two-phase frictional pressure drop and quality. In particular, the frictional pressure drop is reduced to the pressure drop of the single-phase flow by using the definitions developed by Lockhart, Martinelli [1949] as given below:

$$\left(\frac{dp}{dz}\right)_f = \Phi_l^2 \left(\frac{dp}{dz}\right)_l \tag{3.35}$$

Where

$$\left(\frac{dp}{dz}\right)_l = -f \frac{1}{d} \frac{\dot{m}^2}{2\rho_l} \tag{3.36}$$

The liquid-phase mass flow and friction factors are:

$$\dot{m}_l = \dot{m} (1 - x) \quad \text{And} \quad f_l = 0.0316 Re_l^{-0.25} \quad \text{For } 2400 < Re < 3*10^6 \tag{3.37}$$

The liquid phase multiplier, Φ_l is a correction factor for the frictional pressure drop of the single phase and can be defined as a function of the Martinelli parameter given by Martinelli [1949] X_{tt} as:

$$\Phi_l^2 = 1 + \frac{8}{X_{tt}} + \frac{1}{X_{tt}^2} \tag{3.38}$$

Where

$$X_{tt} = \frac{m_l}{m_v} \sqrt{\left(\frac{\rho_v}{\rho_l}\right)} \tag{3.39}$$

The gravitational pressure drop is given by the following equation

$$\left(\frac{dp}{dz}\right)_g = \left[\alpha\rho_v + (1 - \alpha) \rho_l\right] g \tag{3.40}$$

The pressure drops due to acceleration results from the change in momentum of the two phases during the condensation process where pressure gain and heat loss take place. It can be expressed in terms of the elemental inlet and outlet density as:

$$\Delta P_a = (P_o - P_i)_a = G^2 \left[\frac{1}{\rho_o} - \frac{1}{\rho_i} \right] \tag{3.41}$$

The elemental pressure drop can be written as:

$$\Delta P_{ele} = P_{out,ele} - P_{in,ele} = \Delta P_f + \Delta P_g + \Delta P_a \tag{3.42}$$

The total pressure loss and heat transfer is simply the sum of all elemental pressure losses and heat transfer, which are updated after each iteration.

$$\Delta P_{tot} = \sum \Delta P_{ele} \tag{3.43}$$

$$\dot{Q}_{tot} = \sum \dot{Q}_{ele} \tag{3.44}$$

The computation process is repeated for subsequent elements where the inlet conditions of the current element are equal to the outlet conditions of the previous element, namely:

$$(T_i, P_i, \rho_i, q_{ref,i}, E_{h,i})_i = (T_{o,} P_o, \rho_o, q_{ref,o}, E_{h,o})_{i-1} \tag{3.45}$$

This yields the computation of the condenser capacity and pressure drop.

3.2 Geometrical Data and Design Parameters

As this work is concerned with simulation of hot-wall condenser, design details of a hot-wall condenser are required. Therefore all the geometrical data has been taken from an experimental setup taken by Bansal and Chin [2002]. The geometrical data used for simulation are as follows:

Tubing material	stainless steel coated with copper.
Outer diameter of tube	= 0.00475[m]
Inner diameter of tube	= 0.004[m]
Total length of tube in back panel	= 9.64[m]
Length of back panel used for desuperheating	= 0.71 [m]
Length of tube in base panel	= 2.50[m]
Length of tube in right hand side panel	= 5.71[m]
Length of tube in left hand side panel	= 2.86[m]
Length of tube in cross rail	= 2.50[m]
Area of back panel	= 0.8736[m^2]
Area of base panel	= 0.13[m^2]
Area of single (left and right) side panel	= 1.590[m^2]
Area of cross rail panel	= 0.2256[m^2]
Cross sectional area of tube	= 0.00001256[m^2]
Height of the back panel	= 1.4[m]
Height of the single side panel	= 1.656 [m]

3.3 Some Design Parameters

There are some design parameters, which are used in the simulation. These are as follows:

3.3.1 Emissivity of the plate

For the calculation of radiative heat transfer coefficient as discussed in chapter 3, to know the value of emissivity of the plate is essential. These values are taken from “heat and mass transfer data book” by Kothadaraman and Subramanian [2004].

3.3.2 Characteristic length

As discussed by Bansal and Chin [2002] the characteristic length, L_{cha} for a vertical flat surface is equivalent to the height of the plate. So for the back panel and the side panels where the tube are vertical, characteristic length is taken as the height of that panel. And for remaining panels length of the tube is taken as the characteristic length.

3.3.3 Void fraction

The void fraction is one of the most important parameter used to characterize two-phase flows. It is key physical value for determining numerous other important parameters, such as the two phase density and the two phase viscosity and also is of fundamental importance in models for predicting flow pattern transitions, heat transfer and pressure drop. The values of void fractions are taken from "engineering data book iii" by Thome [2004].

3.4 Inlet Conditions at Condenser

For the simulation the inlet conditions are selected as taken by Bansal and Chin [2002], which are 25°C ambient temperature and 40°C refrigerant temperature. Mass flow rate of refrigerant is taken 0.001 kg/s and the quality of refrigerant is kept 0.999. But the quality has to be superheated at the inlet of condenser. Desuperheating length of the tube is also calculated by the same model which is used for the simulation. These conditions are selected for the analysis purpose and by this analysis heat transfer coefficients, pressure drop and heat rejected in condenser can be found.

First the analysis is done for the back panel and then for the base panel. The output conditions of the back panel are to be selected as the input conditions of the base panel. Likewise the complete analysis is done up to left side panel.

The complete analysis is done for two refrigerants; R134a and R12. The input conditions are kept same for all the refrigerants.

3.5 Simulation

The simulation of condenser is carried out by writing various governing equations, described in the preceeding sections on modeling, in the equation window of Engineering Equation Solver (EES). The detailed discussion on EES has been given in section 2.5, chapter 2. The thermodynamic and physical properties of the refrigerants are in built in EES which can be calculated by calling the property subroutines.

The total length of the condenser has been divided in five panels viz., back panel, base panel, right hand side panel, cross rail and left hand side panel. First the simulation of back panel has been carried out and the state of the refrigerant at the outlet of back panel has been taken as input conditions for base panel. Similarly, the simulation of other panels has been carried out successively.

Condenser capacity has been calculated by summing up the heat rejected in all the panels. Average value of various heat transfer coefficients has been calculated for each panel at the average conditions.

A sample program written in Engineering Equation Solver has been appended in Appendix C along with sample results.

Chapter 4

RESULTS AND DISCUSSION

The results of simulation and discussions thereof have been presented in this chapter.

4.1 Simulation of Hot-wall Condenser for R134a and R12 Refrigerants

In the hot wall condenser, as there are five panels, refrigerant coming from the compressor first goes to the back panel directly. From the back panel it goes to base panel then to right side panel. In the end it goes to left side panel which is connected to right side panel by a cross rail. The simulation has been carried out for R134a and R12 refrigerants and the results have been presented in tables and plotted in figures for both the refrigerants for comparison.

4.1.1 Analysis of the all panels

For the two refrigerants analysis is done for all the panels. Computation is done by taking complete panel length as one element. The output of the one panel is taken as input to the adjacent panel.

4.1.1.1 Input conditions for the different panels

Input conditions for the two refrigerants in different panels are given in the Table 4.1 and Table 4.2. All this analysis is done for the mass flow rate of 0.001 kg/s and ambient temperature of 298 K.

Table 4.1 Input conditions for R134a in each panel

Panel	Temperature (K)	Quality (x)	Pressure (kPa)	Density (kg/m^3)	Enthalpy (kJ/kg)
Back	313.0	0.9990	1012.5	50.35	417.73
Base	312.6	0.2970	895.7	150.72	304.18
Right	309.4	0.2733	893.1	149.30	296.46
Cross rail	307.9	0.2066	886.8	182.75	283.44
Left	303.8	0.1892	883.8	277.63	275.29

Table 4.2 Input conditions for R12 in each panel

Panel	Temperature (K)	Quality (x)	Pressure (kPa)	Density (kg/m^3)	Enthalpy (kJ/kg)
Back	313.0	0.9990	955.29	54.734	367.61
Base	312.5	0.5109	846.90	100.81	304.96
Right	309.4	0.4646	845.00	101.91	296.82
Cross rail	307.9	0.3817	840.20	117.59	284.71
Left	303.9	0.3424	837.80	117.77	276.29

4.1.1.2 Output conditions for the different panels

Output conditions for both the refrigerants in all the panels are given in the Table 4.3 and Table 4.4.

Table 4.3 Output conditions for R134a in each panel

Panel	Temperature (K)	Quality (x)	Pressure (kPa)	Density (kg/m^3)	Enthalpy (kJ/kg)
Back	312.6	0.2970	895.7	150.72	304.18
Base	309.4	0.2733	893.1	149.30	296.46
Right	307.9	0.2066	886.8	182.75	283.44
Cross rail	303.8	0.1892	883.8	277.63	275.29
Left	298.2	0.0083	879.8	927.53	236.09

Table 4.4 Output conditions for R12 in each panel

Panel	Temperature (K)	Quality (x)	Pressure (kPa)	Density (kg/m^3)	Enthalpy (kJ/kg)
Back	312.5	0.5109	846.9	100.81	304.96
Base	309.4	0.4646	845.0	101.90	296.82
Right	307.9	0.3817	840.2	117.59	284.70
Cross rail	303.9	0.3424	837.8	117.77	276.29
Left	298.1	subcool	834.8	1311.00	224.01

4.1.1.3 Results of simulation

All the desired parameters obtained by the simulation for both the refrigerants are given in the Table 4.5 and Table 4.6.

Table 4.5 Results for R134a in each panel

Panel	Convective heat transfer coefficient (W/m^2-K)	Radiative heat transfer coefficient (W/m^2-K)	Outer heat transfer coefficient (W/m^2-K)	Inner heat transfer coefficient (W/m^2-K)	Pressure drop (kPa))	Heat rejected in condenser (W)	Overall heat transfer coefficient (W/m^2-K)
Back	2.347	5.545	7.892	2074	116.8	100.20	7.862
Base	1.213	3.210	4.424	1092	2.6	7.10	4.406
Right	2.042	5.415	7.457	1071	6.3	8.30	7.405
Cross rail	0.902	3.190	4.092	964	3.0	5.90	4.075
Left	0.778	5.160	6.022	950	4.0	65.80	5.902

Total heat rejected in condenser = 187.3 W

Table 4.6 Results for R12 in each panel

Panel	Convective heat transfer coefficient (W/m^2-K)	Radiative heat transfer coefficient (W/m^2-K)	Outer heat transfer coefficient (W/m^2-K)	Inner heat transfer coefficient (W/m^2-K)	Pressure drop (kPa)	Heat rejected in condenser (W)	Overall heat transfer coefficient (W/m^2-K)
Back	2.343	5.542	7.885	1623	108.4	99.34	7.847
Base	1.213	3.210	4.424	1109	1.9	7.56	4.406
Right	2.042	5.415	7.457	1077	4.8	8.80	7.405
Cross rail	0.906	3.190	4.096	984	2.3	6.80	4.079
Left	0.778	5.160	5.939	958	3.0	69.60	5.902

Total heat rejected in condenser = 192.1 W

From this analysis, it can be seen that how refrigerant is condensed in successive panels. The quality at the inlet of back panel is 0.999 for both the refrigerants which is almost saturated vapour condition and final condition for R134a at outlet of left side panel is

coming 0.01 dry which is almost saturated liquid condition, however for R12, the final condition at outlet of left side panel is coming subcooled liquid state.

4.1.2 Effect of ambient temperature on various parameters for R134a and R12

Ambient temperature is the important parameter for the designing purpose, because this depends on the surroundings or nature, which is always changing. Hence, an investigation is essential to study the effect of ambient temperature. The study is done for both the refrigerants in the range between the temperature lower than the outlet temperature of that panel and above that temperature for which temperature at outlet converges.

The study is done for all the panels and the effect of this operating parameter on inner and outer heat transfer coefficients and the condenser heat capacity has been studied. Results are presented in tables and figures for all the panels.

4.1.2.1. Study of the back panel

Refrigerant coming from compressor first goes towards back panel of the condenser**.** From the program, which is written in EES, it can be seen that outlet temperature of this panel is 312.6 K and the program converges up to 293 K for refrigerant R134a. So the effect of ambient temperature has been seen by varying it from 312 K to 293 K, which is shown in the Table A1 and Figs. 4.1 to 4.4.

The outlet temperature of this panel is obtained 312.5 K for R12 and the program converges up to 290 K. So the effect of ambient temperature has been seen by varying it from 312.5 K to 290 K, which is shown in the Table B1 and Figs. 4.1 to 4.4.

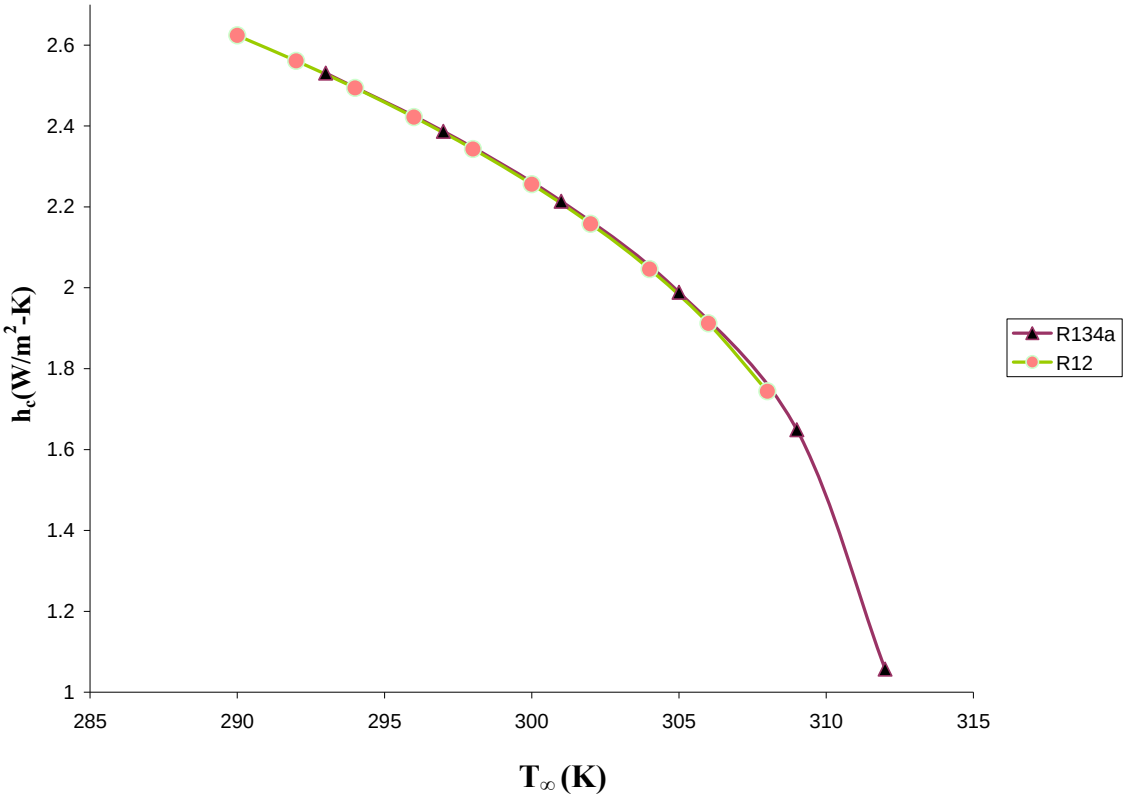

Fig.4.1 Effect of ambient temperature on convective heat transfer coefficient (back panel)

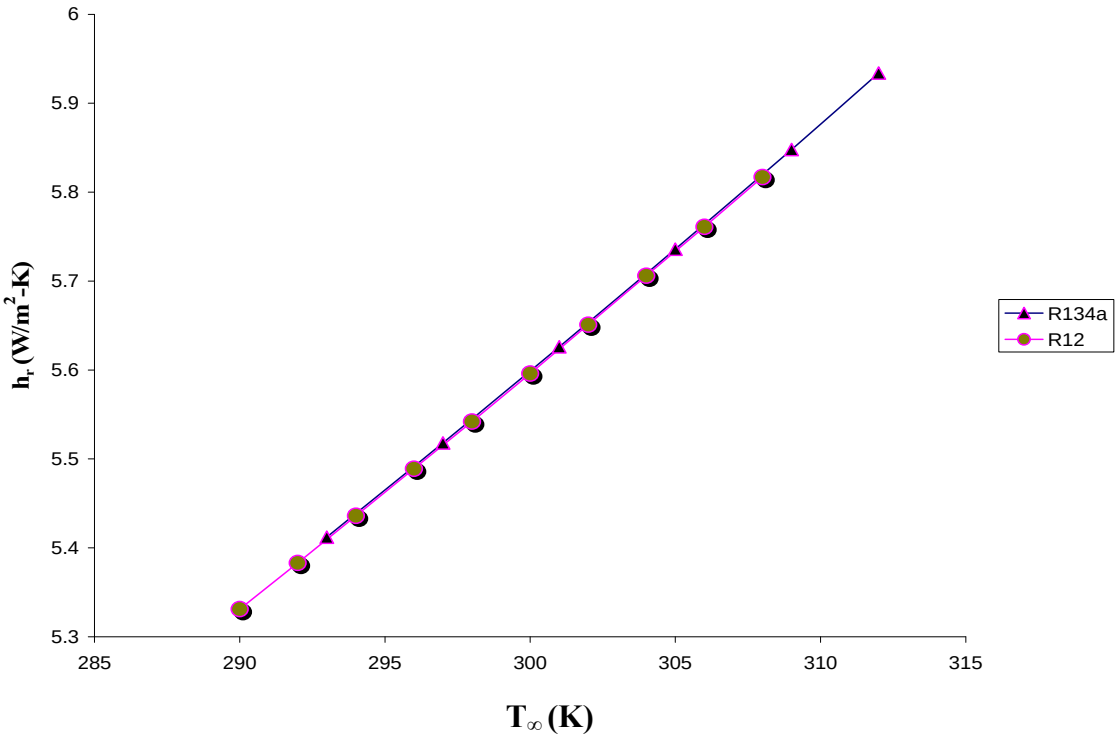

Fig.4.2 Effect of ambient temperature on radiative heat transfer coefficient (back panel)

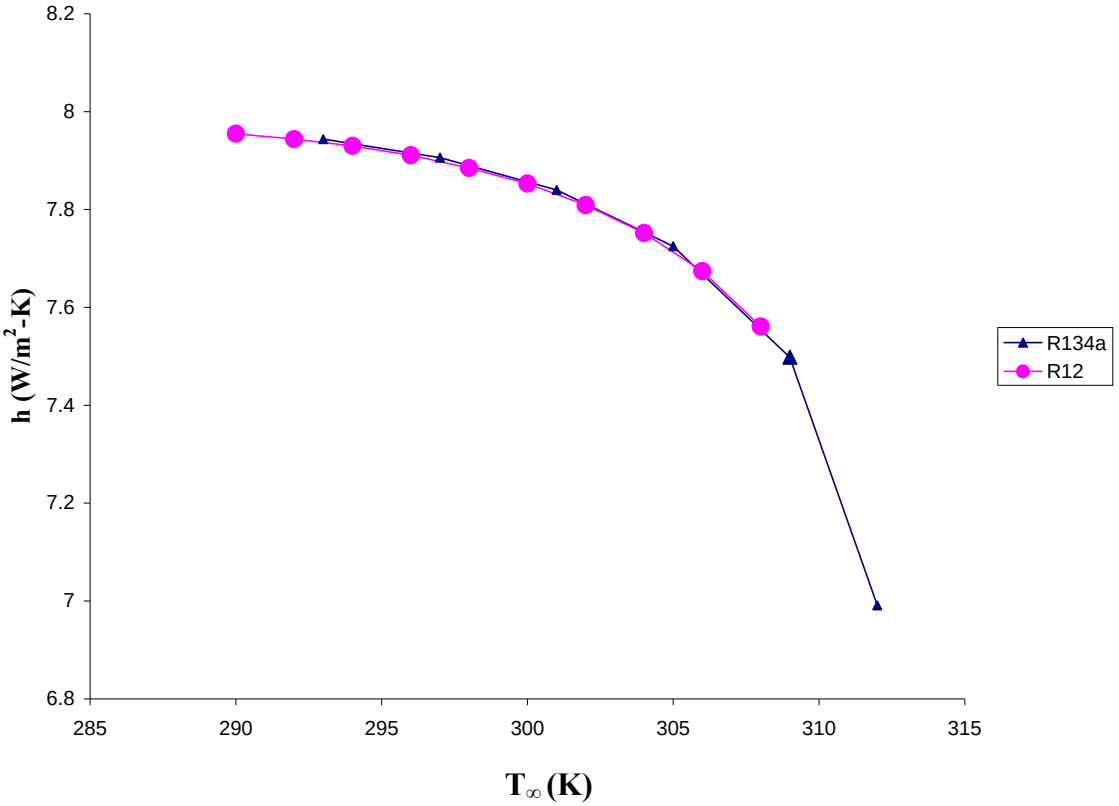

Fig.4.3 Effect of ambient temperature on outer heat transfer coefficient (back panel)

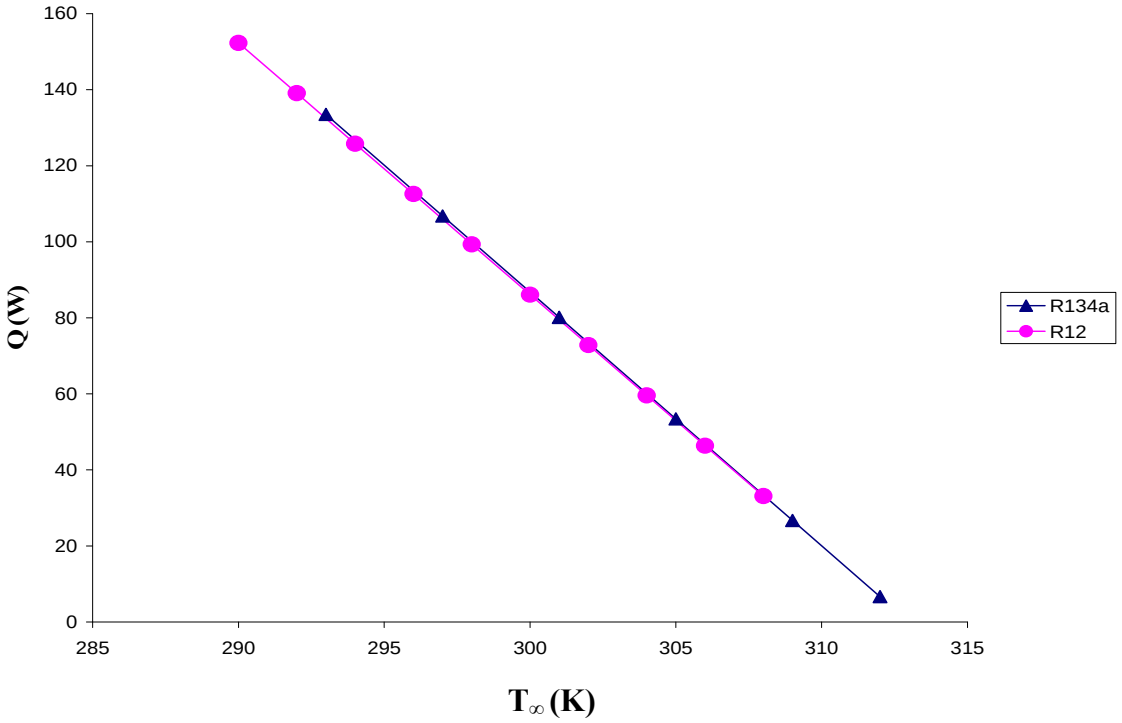

Fig. 4.4 Effect of ambient temperature on heat rejected (up to back panel)

It can be seen from the Tables A1 and B1 and Figs. 4.1 to 4.4, only outer heat transfer coefficient which is the sum of convective and radiative heat transfer coefficients is affected by the ambient temperature. Inner heat transfer coefficient is constant for all the ambient conditions. It has been seen that most of the drop in quality (0.693 for R134 and 0.479 for R12) is occurring in this panel only because it has largest tube length and surface area and also having largest inside heat transfer coefficient.

4.1.2.2 Study of the base panel

Refrigerant goes to base panel from the back panel. The temperature of the ambient is taken 5 K more because this panel faces the ground. In this panel outlet temperature is 309.4 K for R134a and the program converges up to 293 K. So the effect of ambient temperature has been seen by varying it from 309.4 K to 293 K, which is shown in the Table A2 and Figs. 4.5 to 4.8.

For R12, outlet temperature is 309.4 K in this panel and the program converges up to 291 K. So the effect of ambient temperature has been seen by varying it from 309.4 K to 291 K, which is shown in the Table B2 and Figs. 4.5 to 4.8.

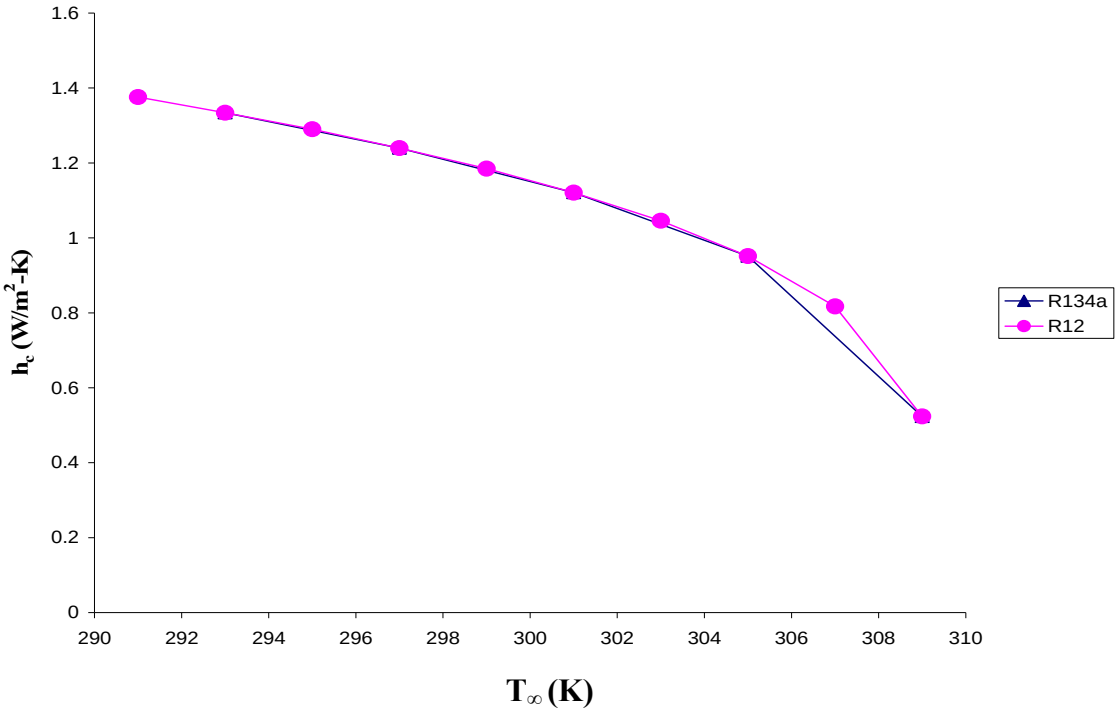

Fig.4.5 Effect of ambient temperature on convective heat transfer coefficient (base panel)

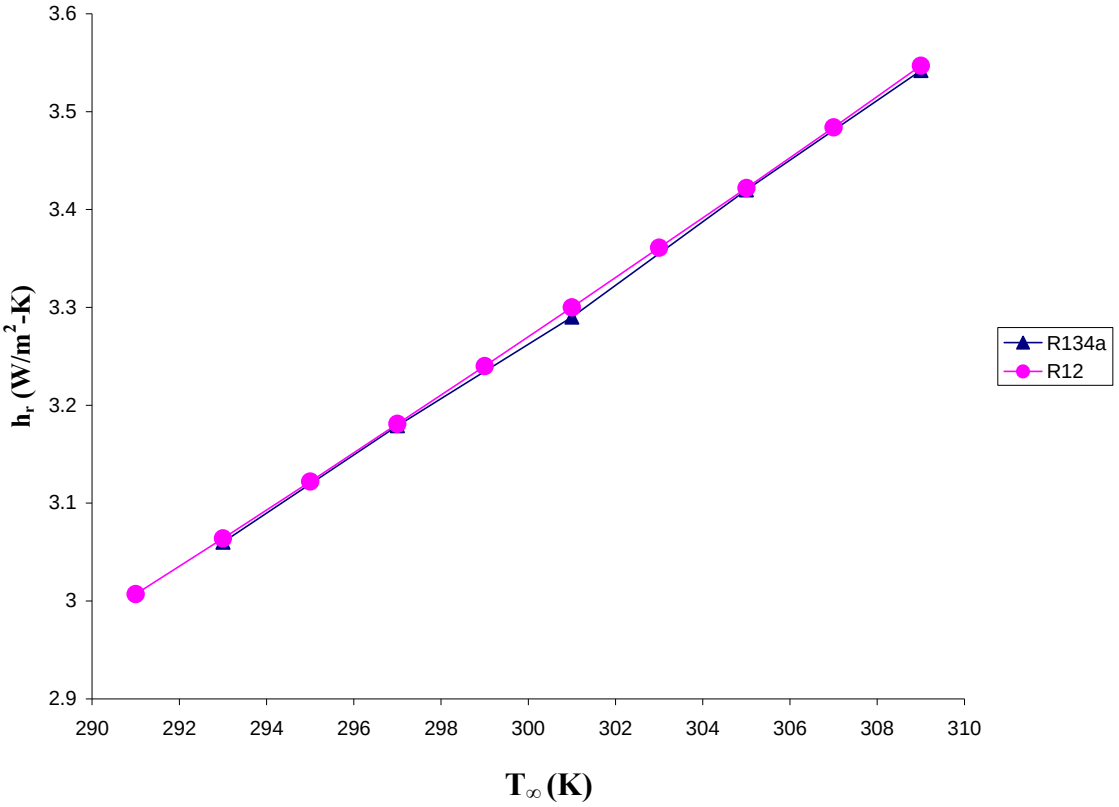

Fig.4.6 Effect of ambient temperature on radiative heat transfer coefficient (base panel)

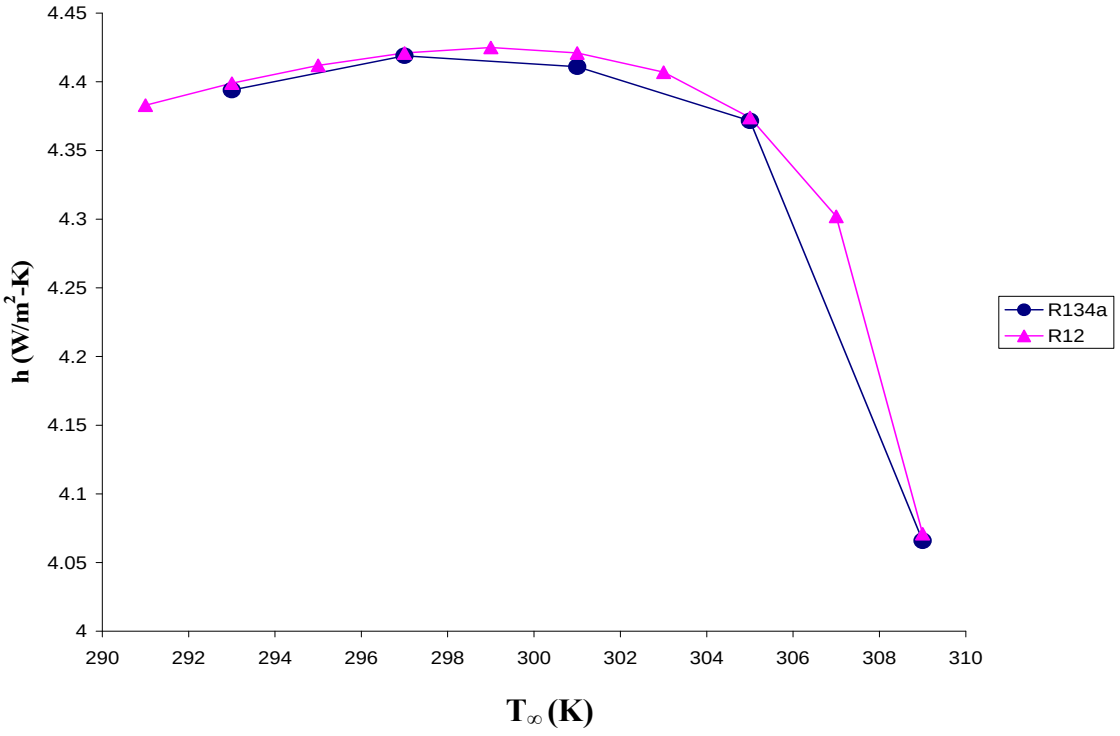

Fig.4.7 Effect of ambient temperature on outer heat transfer coefficient (base panel)

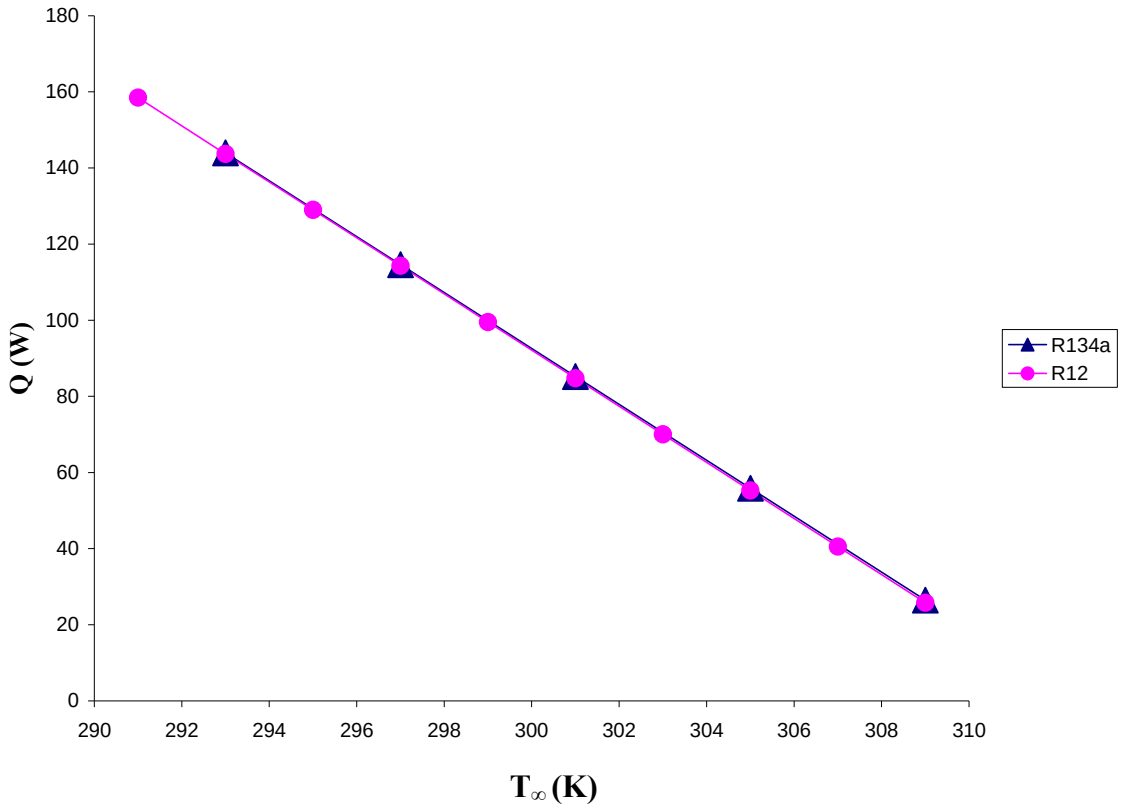

Fig.4.8 Effect of ambient temperature on total heat rejected (up to base panel)

It can be seen that from the Figs. 4.5 to 4.8 and tables A2 and B2 that heat transfer coefficients are reduced a lot and this is because of short tube length of base panel and less surface area of the base panel. Inner heat transfer coefficient is remaining constant for all the ambient condition. Because of less heat transfer coefficients the drop in quality is very less. The quality at the outlet is found to be 0.2733 for R134a and 0.4646 for R12.

4.1.2.3 Study of the right hand side panel

Refrigerant goes to right hand side panel from the base panel. The output temperature in this panel for R134a is 307.9 K and program converges up to 296 K. Hence the effect of ambient temperature has been seen by varying it from 307.9 K to 296 K. This is shown in Table A3 and Figs. 4.9 to 4.12.

The output temperature in this panel for R12 is 307.9 K and the program converges up to 289 K. Hence the effect of ambient temperature has been seen by varying it from 307.9 K to 289 K. This is shown in Table B3 and Figs. 4.9 to 4.12.

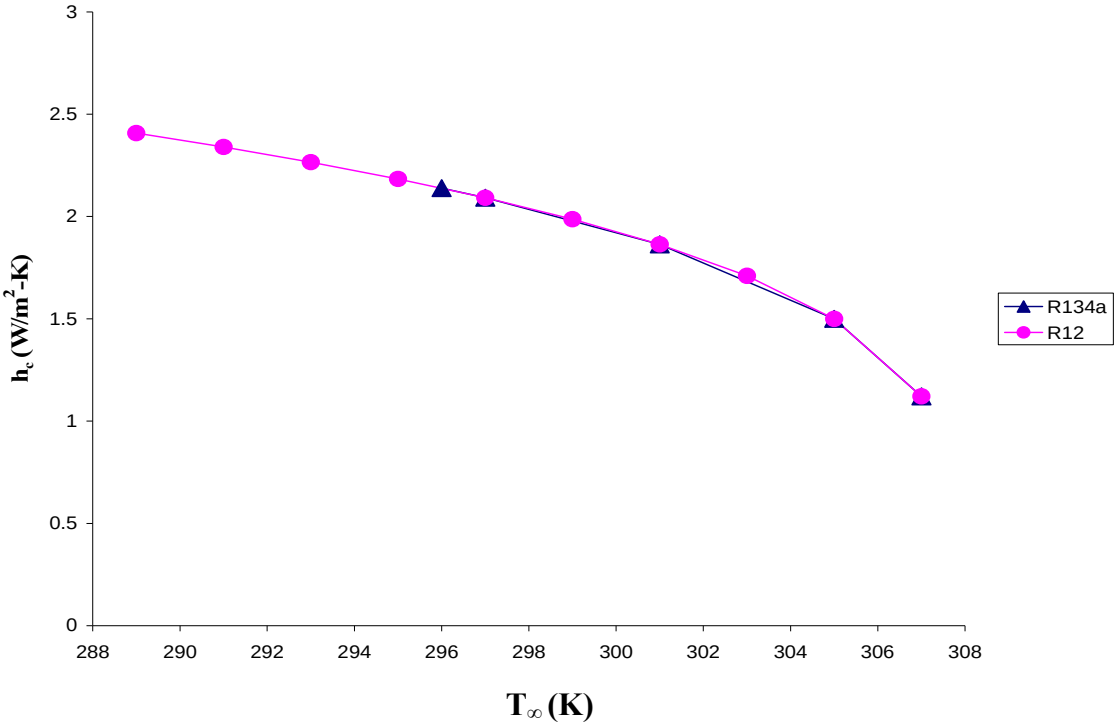

Fig.4.9 Effect of ambient temperature on convective heat transfer coefficient (right side panel)

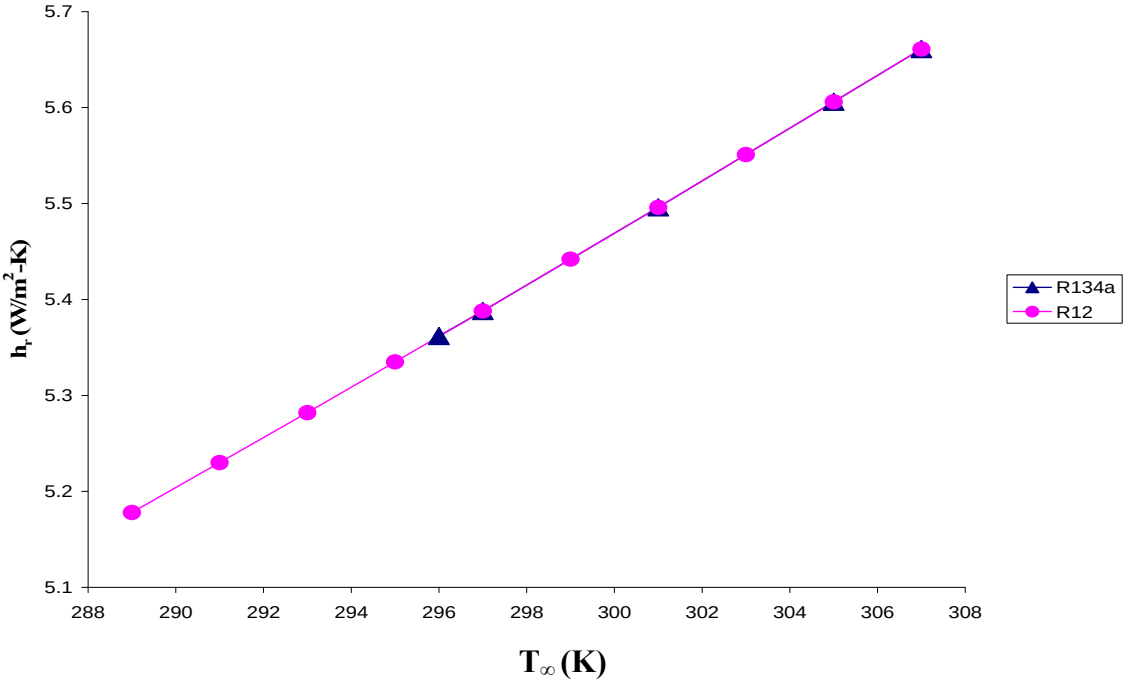

Fig.4.10 Effect of ambient temperature on radiative heat transfer coefficient (right side panel)

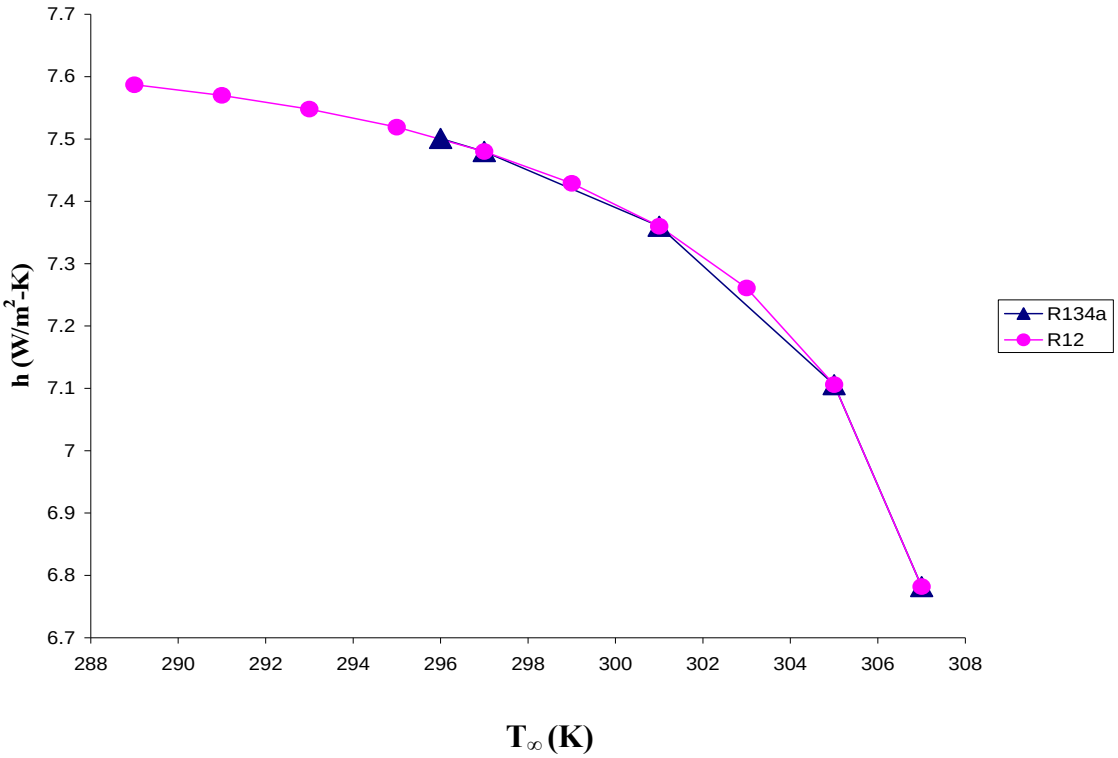

Fig.4.11 Effect of ambient temperature on outer heat transfer coefficient (right side panel)

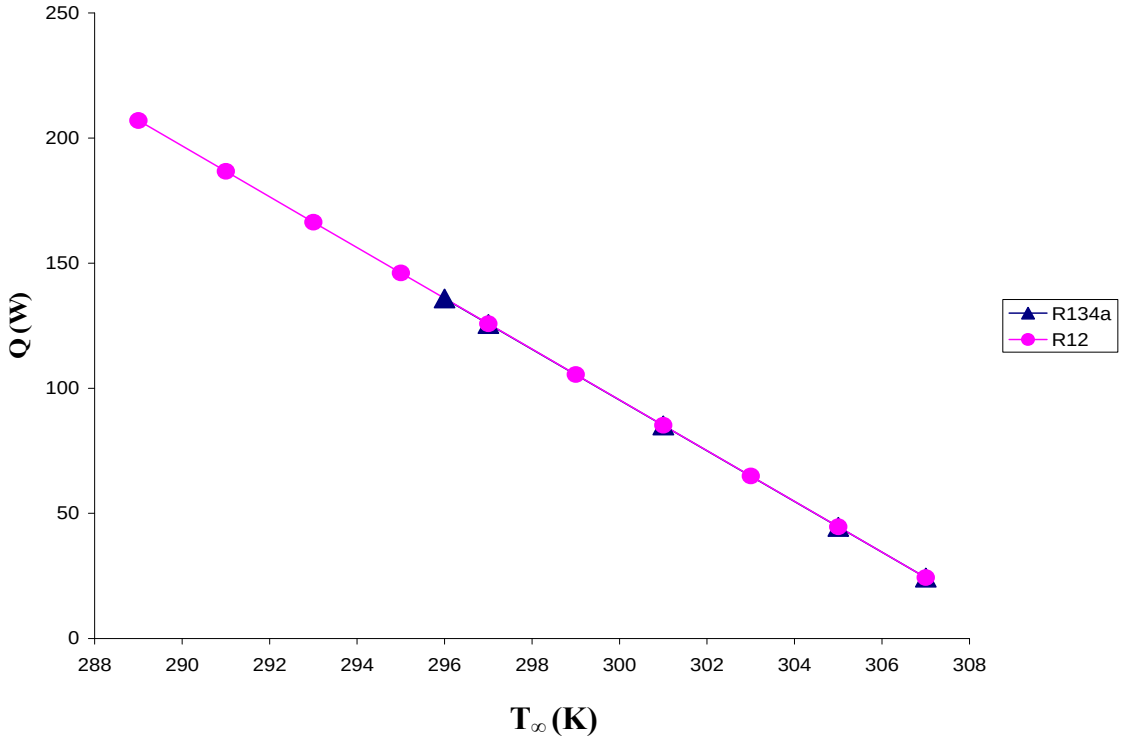

Fig.4.12 Effect of ambient temperature on total heat rejected (up to right side panel)

From the Figs. 4.9 to 4.12, it can be seen that how all the parameters depend upon ambient temperature for both the refrigerants. Here the drop in quality is significant and quality at outlet is found to be 0.2066 for R134a and 0.3817 for R12.

4.1.2.4 Study of the cross rail

After passing from right hand side panel refrigerant goes to left side panel by a cross rail which makes possible the connection between these two side panels. Hence the study of cross rail is also essential. The output temperature in this case is 303.8 K for R134a and the program converges up to 296 K. Hence the effect of ambient temperature has been seen by varying it from 303.8 K to 296 K. This is shown in Table A4 and Figs. 4.13 to 4.16.

For R12, the output temperature in this panel is 303.9 K and the program converges up to 294 K. Hence the effect of ambient temperature has been seen by varying it from 303.9 K to 294 K. This is shown in Table B4 and Figs. 4.13 to 4.16.

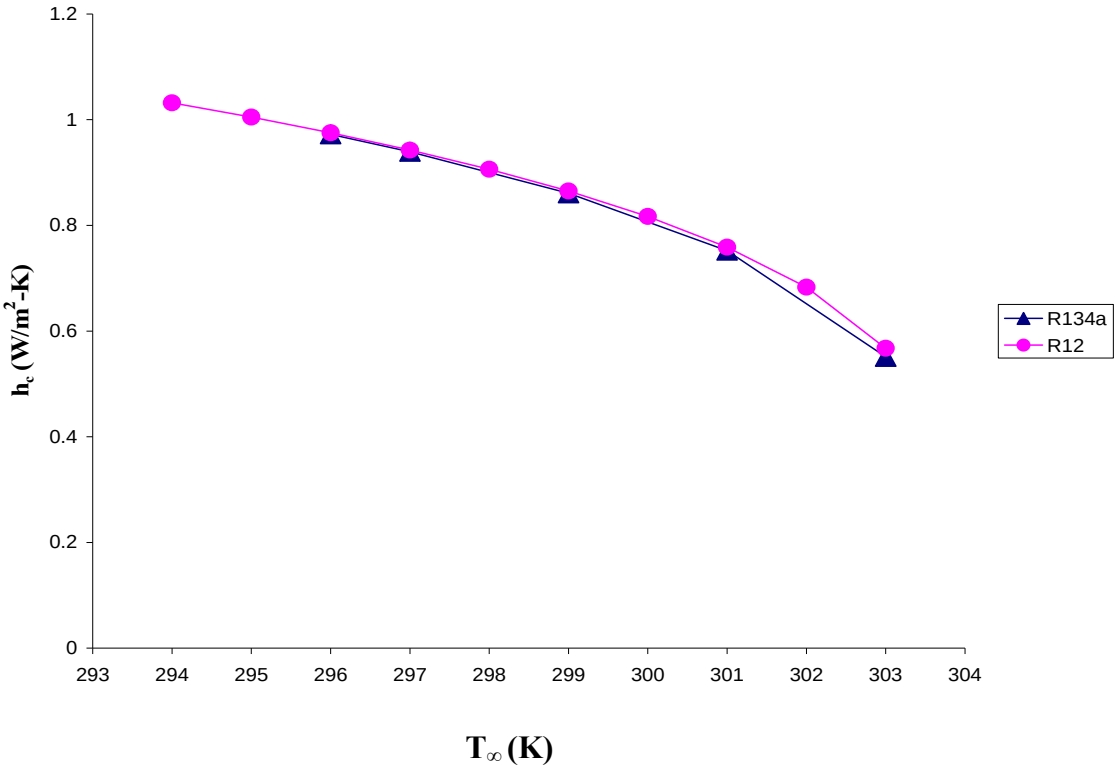

Fig.4.13 Effect of ambient temperature on convective heat transfer coefficient (cross rail)

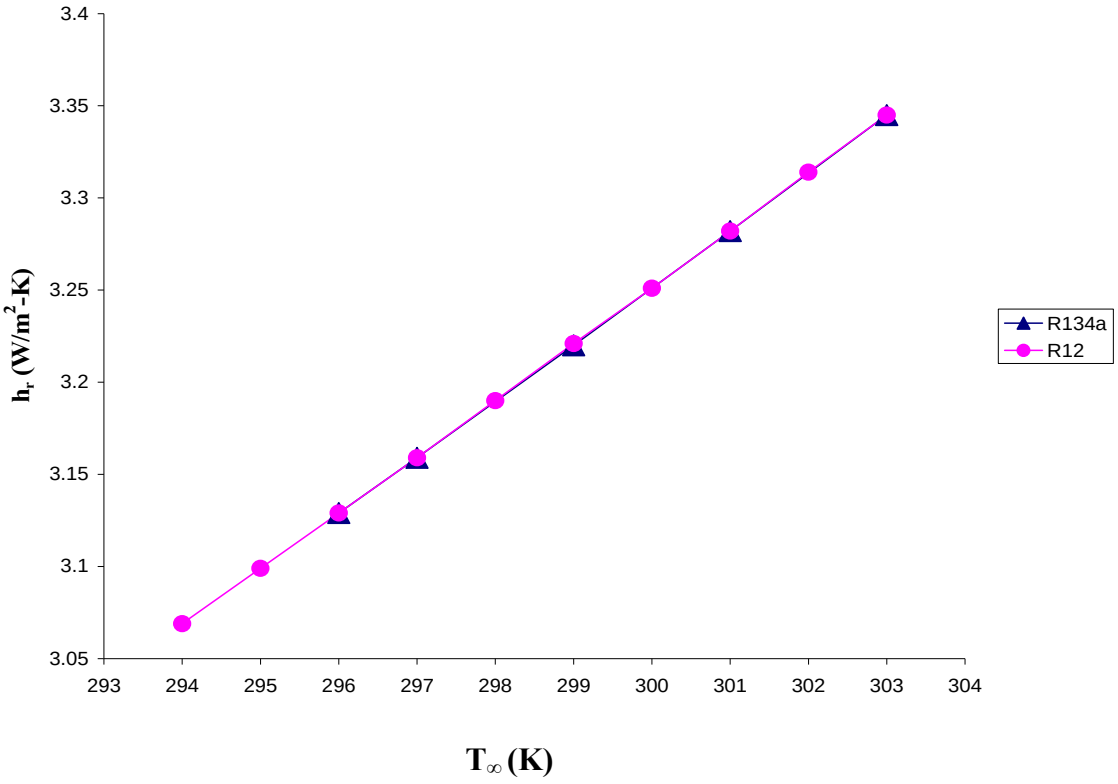

Fig.4.14 Effect of ambient temperature on radiative heat transfer coefficient (cross rail)

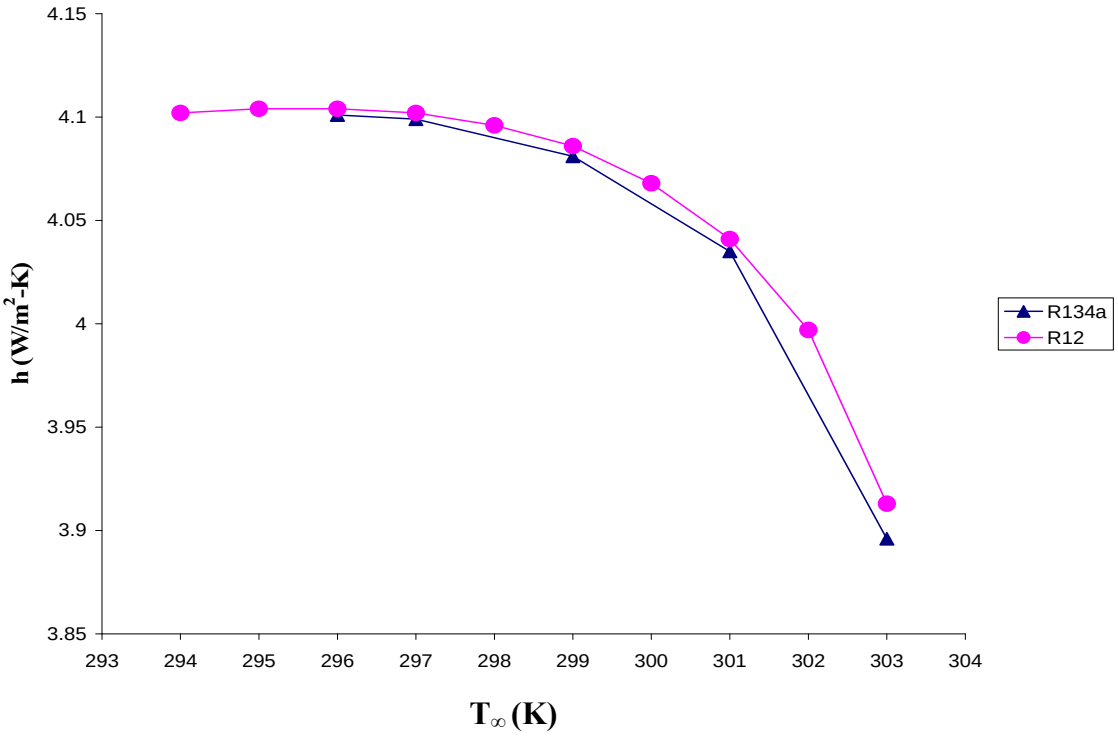

Fig.4.15 Effect of ambient temperature on outer heat transfer coefficient (cross rail)

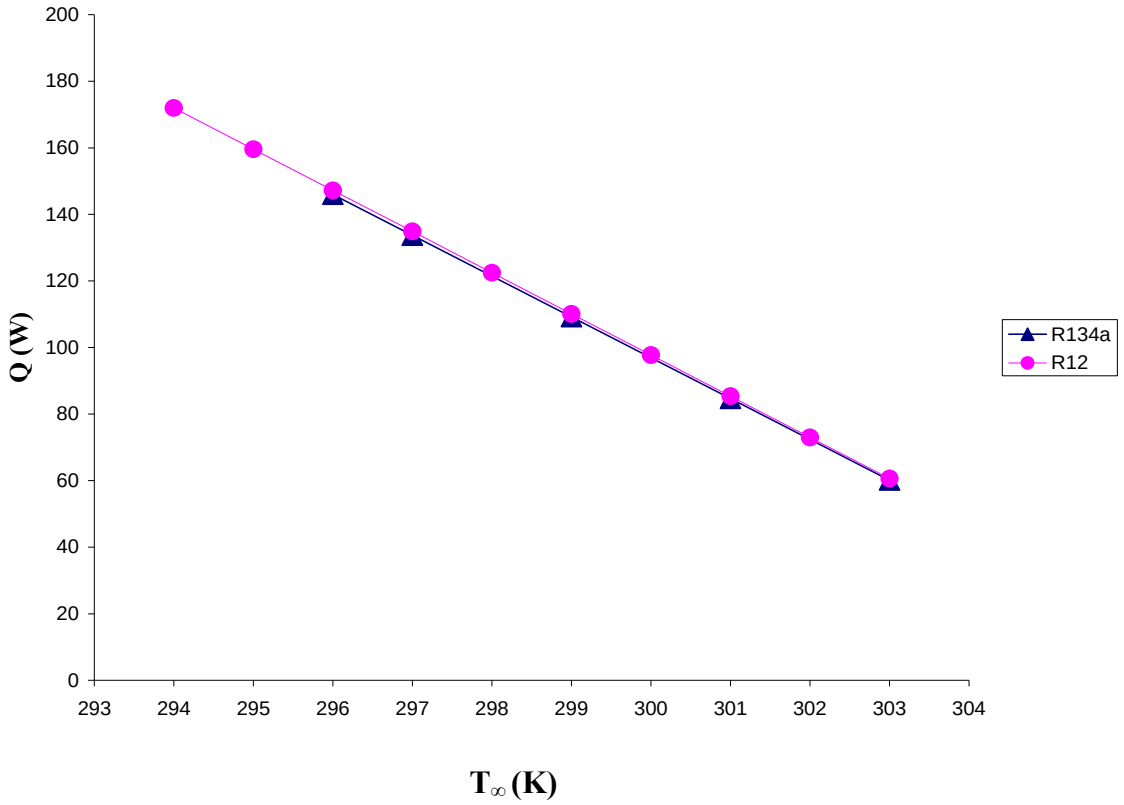

Fig.4.16. Effect of ambient temperature on total heat rejected (up to cross rail)

From the Figs. 4.13 to 4.16, it can be seen that how all the parameters vary with ambient temperature for both the refrigerants. Here the drop in quality is very small and quality at outlet is found to be 0.1892 for R134a and 0.3424 for R12. This is because of lesser length of tube.

4.1.2.5 Study of the left side panel

In the end refrigerant reaches in the left side panel where it is finally condensed to liquid state. In this panel, outlet temperature is 298.2 K for R134a and program converges up to 298 K. Hence, the effect of ambient temperature has been seen by varying it from 298.2 K to 298.1 K. This is shown in the Table A5 and Figs. 4.17 to 4.20.

For R12, outlet temperature is 298.1 K in this panel and program converges up to 289 K. Hence, the effect of ambient temperature has been seen by varying it from 298.2 K to 298.1 K. This is shown in the Table B5 and Figs. 4.17 to 4.20.

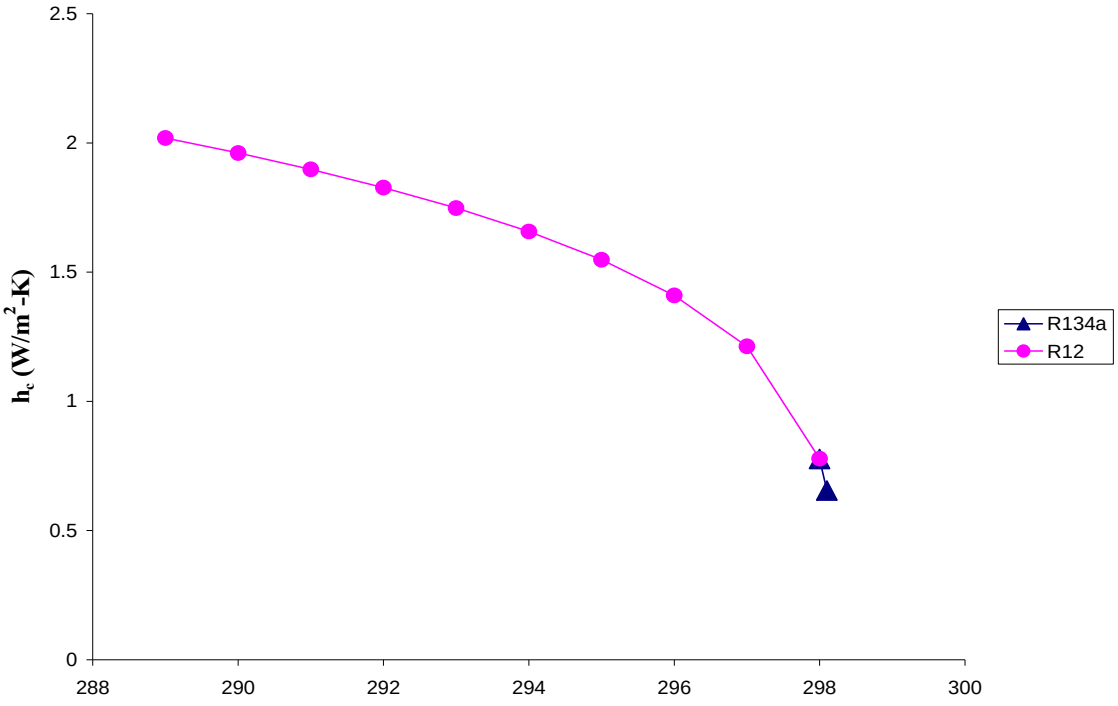

Fig.4.17 Effect of ambient temperature on convective heat transfer coefficient (left side panel)

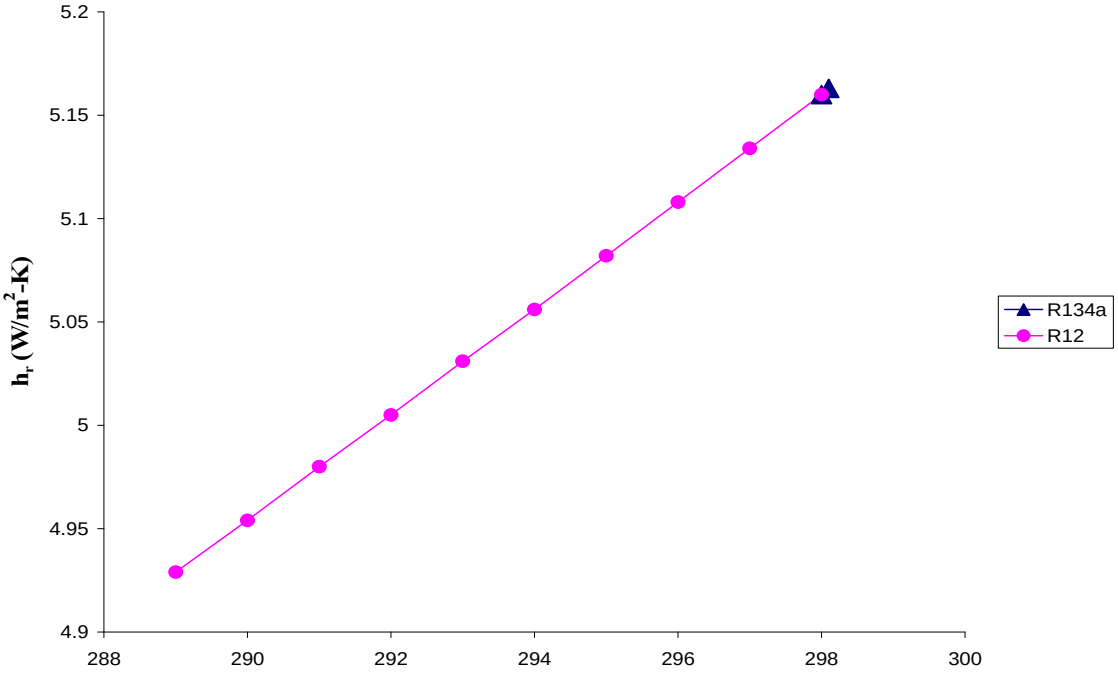

Fig.4.18 Effect of ambient temperature on radiative heat transfer coefficient (left side panel)

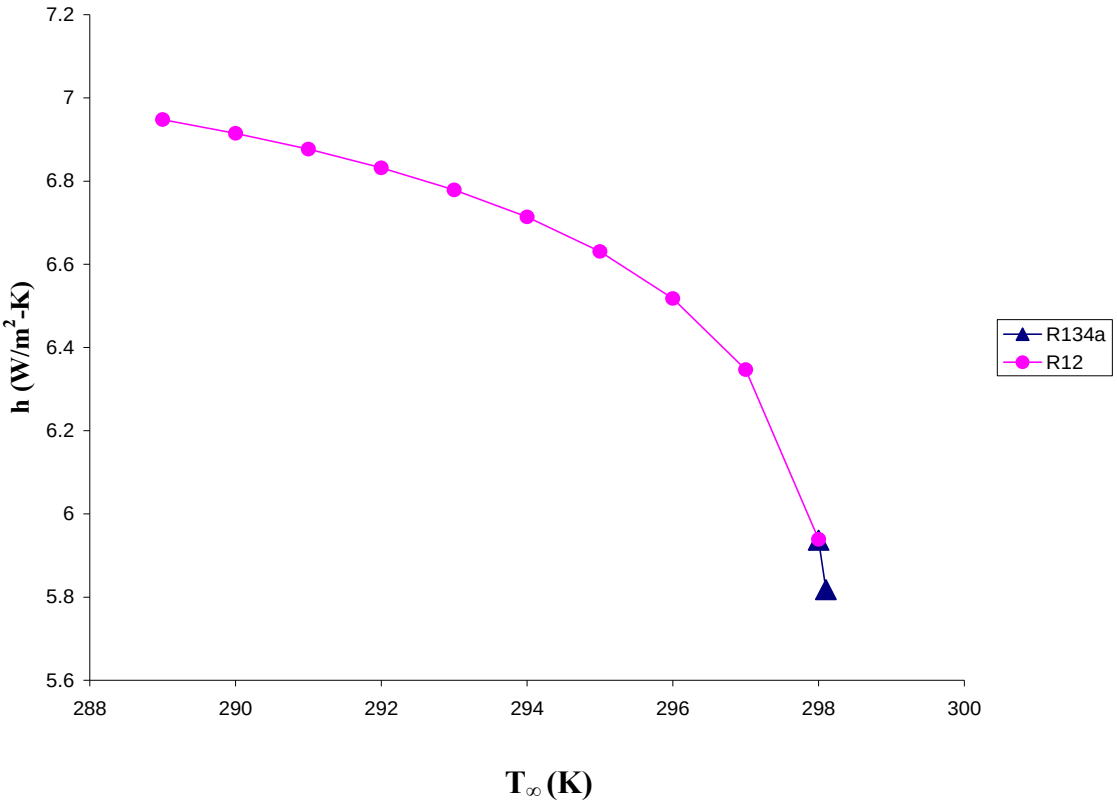

Fig.4.19 Effect of ambient temperature on outer heat transfer coefficient (left side panel)

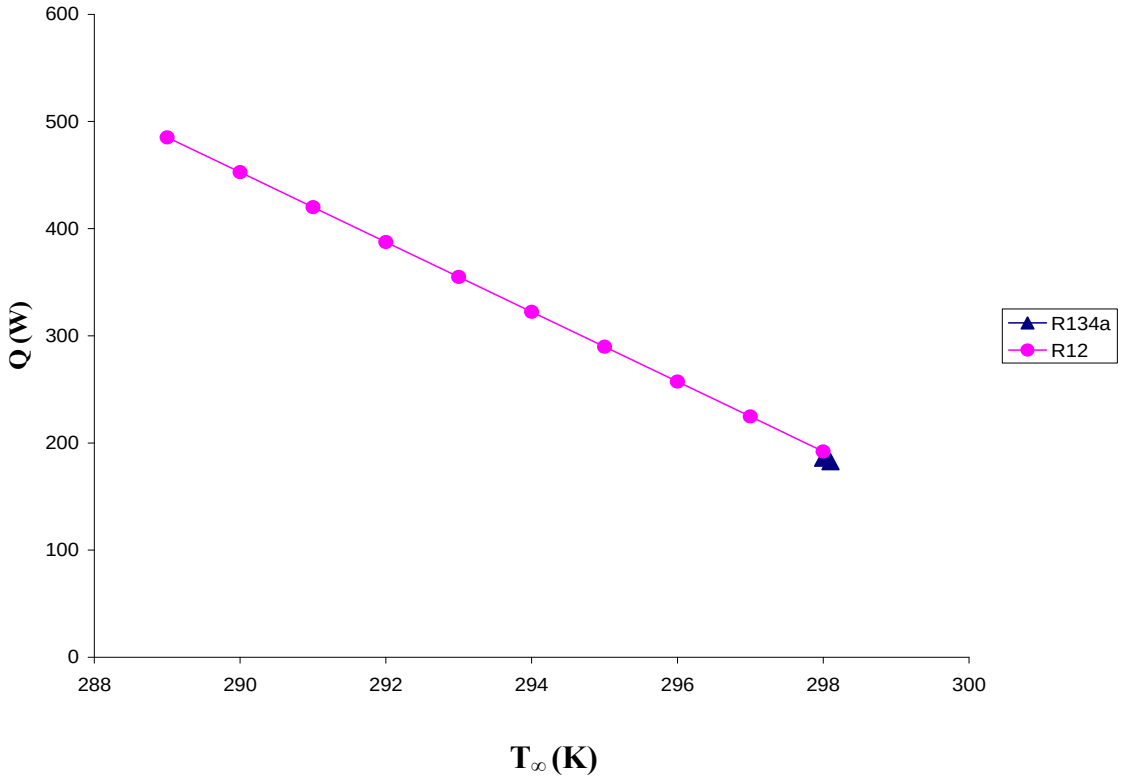

Fig.4.20 Effect of ambient temperature on total heat rejected (up to left side panel)

From the Figs. 4.17 to 4.20, it can be seen that how all the parameters vary wih temperature for both the refrigerants. Here the quality reaches up to 0.0083 for R134a, which is very near to saturated liquid state. For R12 the quality at the outlet is found to be subcooled liquid state.

It can be observed that for all the cases, convective heat transfer coefficient decreases when ambient temperature increases. This is because; as the ambient temperature is increased, the Rayleigh number decreases (Eqn. (3.10)) and also Prandlt number decreases. From Eqn. (3.9) it can be seen that when Rayleigh number and the Prandlt number decreases, Nusselt number also decreases. Hence convective heat transfer coefficient on air side (outside) decreases as ambient temperature increases.

Like this from Eqns. (3.6) and (3.12), it can be seen that as ambient temperature increases, average plate temperature also increases hence radiative heat transfer coefficient increases. Nature of outer heat transfer coefficient with ambient temperature depends upon convective and radiative heat transfer coefficients, because outer heat transfer coefficient is the sum of convective and radiative heat transfer coefficients. The net effect on outer heat transfer coefficient of ambient temperature is that it decreases with ambient temperature as evident from Figs. 4.3, 4.7, 4.11, 4.15 and 4.19.

From Eqn.(3.3), it is also seen that as ambient temperature increases, heat rejected in the panel decreases.

Therefore from this analysis the effect of the ambient temperature on different parameters can be seen. So this study is very helpful in the design of hot-wall condenser.

4.1.3 Effect of mass flow rate on various parameters for R134a and R12

In the design of any type of condenser, study of mass flow rate is essential. Inside heat transfer coefficient (refrigerant side) depends largely upon mass flow rate. Therefore, a study is done by varying mass flow rate from 0.001 kg/s to 0.01 kg/s

4.1.3.1 Study of back panel

All the results are shown in Table A6 for R134a and in Table B6 for R12. For this panel results are converging up to .01 kg/s for R134a and 0.004 kg/s for R12. So the results are obtained in the range of 0.001 kg/s to 0.01 kg/s for R134a and 0.001 kg/s to 0.004 kg/s for R12. This is shown in Figs. 4.21 and 4.22.

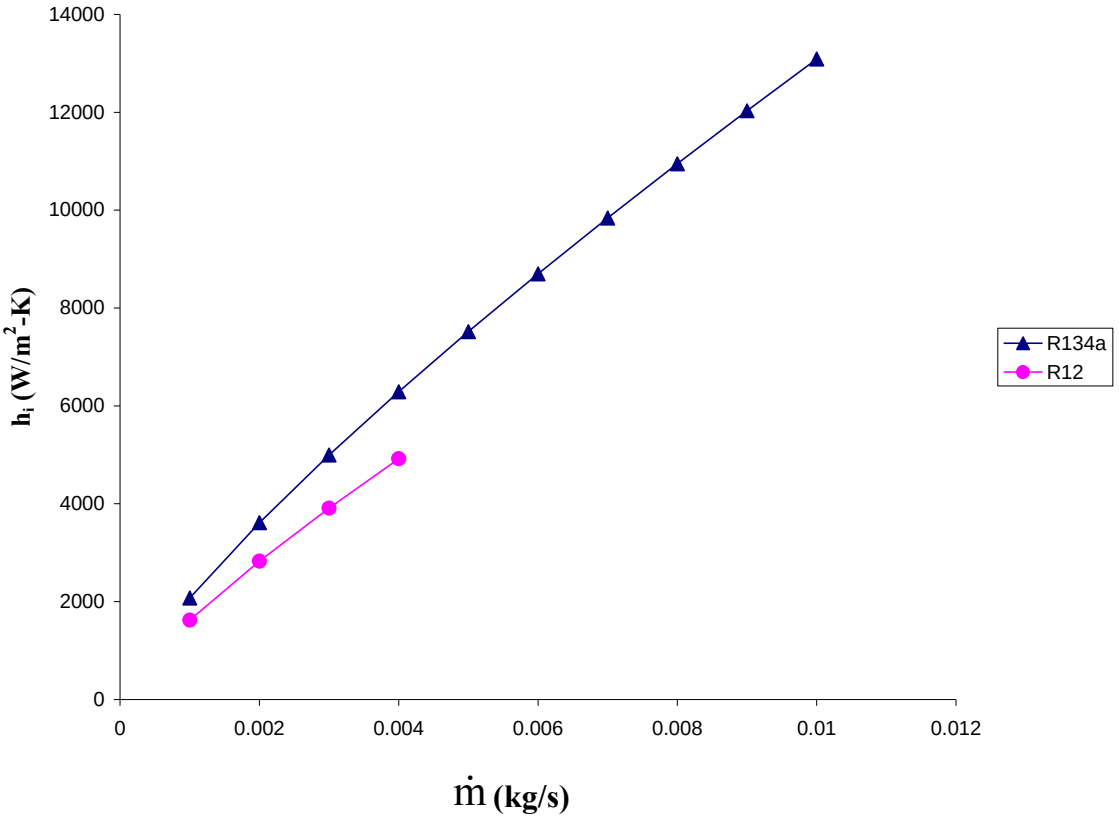

Fig.4.21 Effect of mass flow rate on inner heat transfer coefficient (back panel)

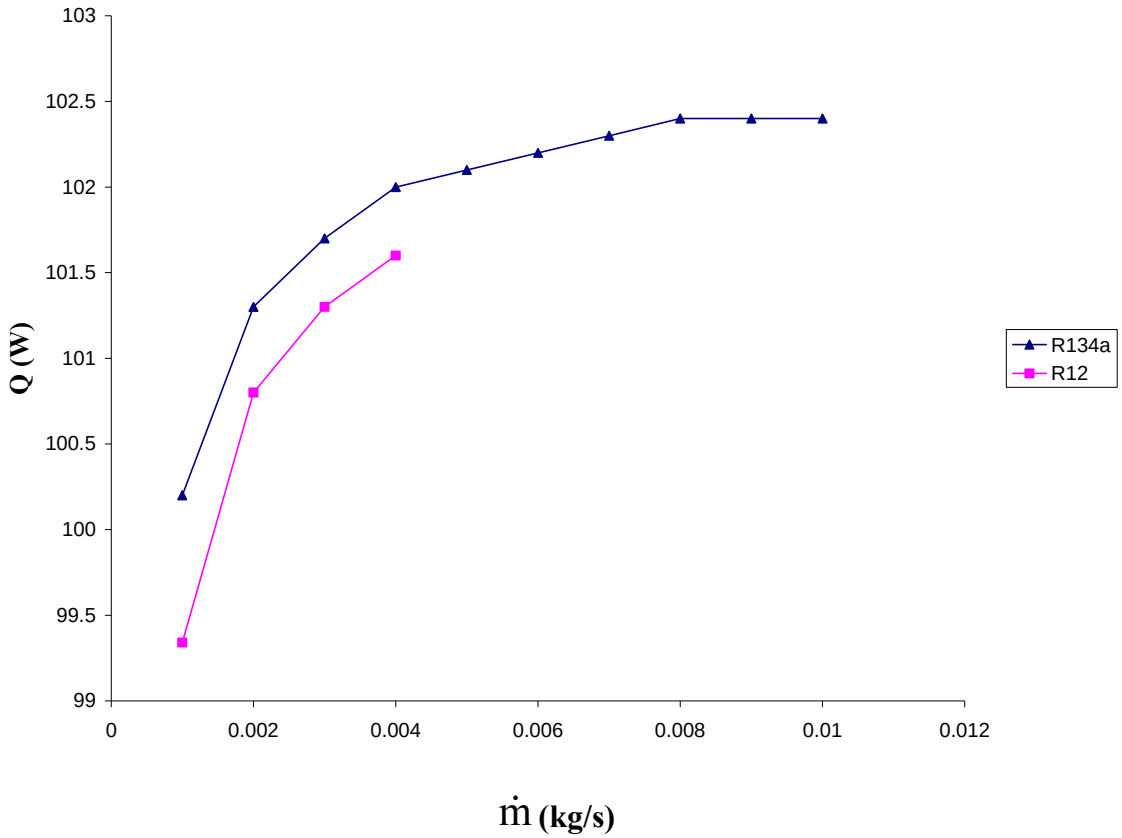

Fig.4.22 Effect of mass flow rate on heat rejected (back panel)

From Table A6 and B6, it can be concluded that only inside heat transfer coefficient increases with mass flow rate. Outer heat transfer coefficient (which is sum of convective and radiative heat transfer coefficient) is constant for the entire mass flow rate because air side conditions are same throughout.

4.1.3.2 Study of base panel

All the results are shown in Table A7 and B7 for both the refrigerants and Figs. 4.23 to 4.24. For this panel results are converging up to .01 kg/s for R134a and 0.005 kg/s for R12. So the results are obtained in the range of 0.001 kg/s to 0.01 kg/s for R134a and 0.001 kg/s to 0.005 kg/s for R12. This is shown in Figs. 4.23 and 4.24.

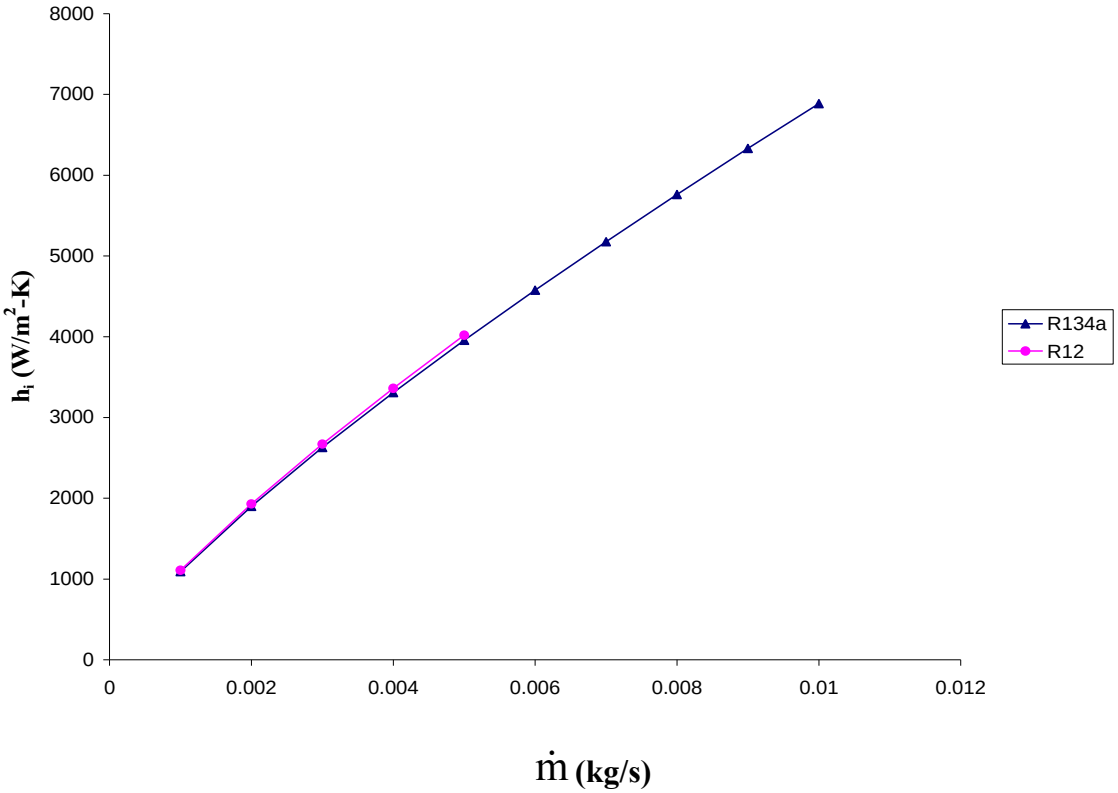

Fig.4.23 Effect of mass flow rate on inner heat transfer coefficient (base panel)

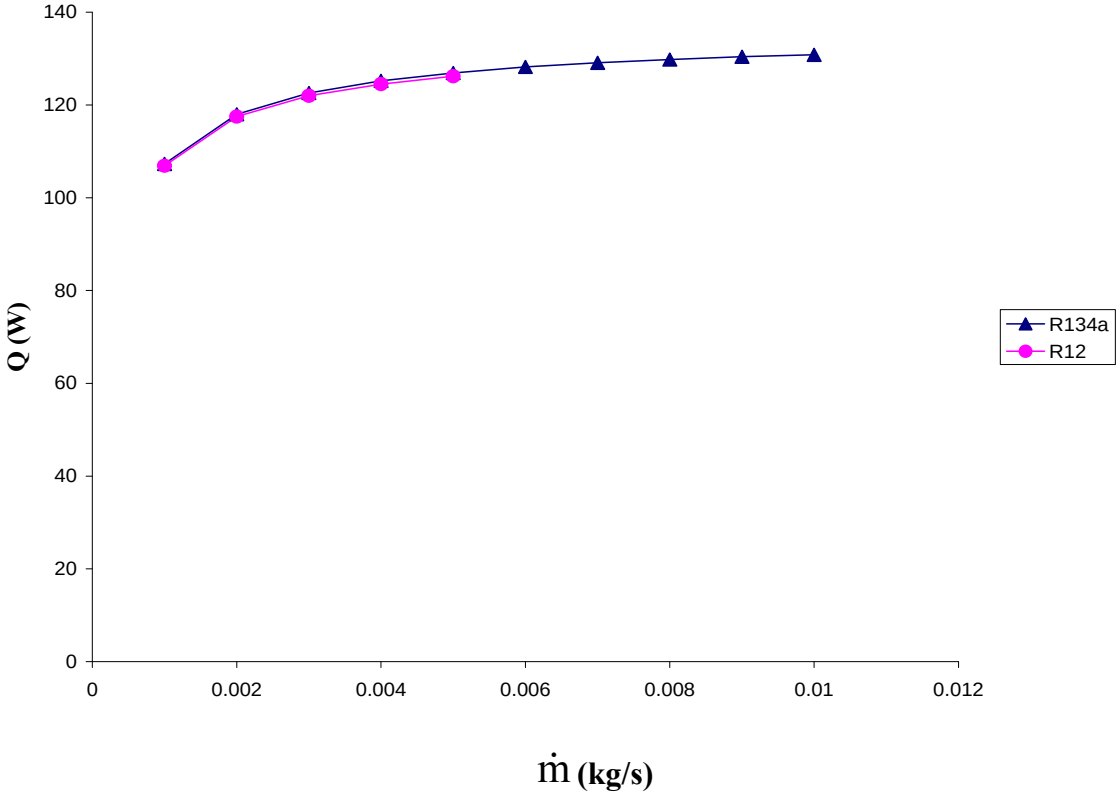

Fig.4.24 Effect of mass flow rate on total heat rejected (up to base panel)

From Table A7 and B7, it can be concluded that only inner heat transfer coefficient depend upon mass flow rate. The behaviour of inner heat transfer coefficient and heat flow rate has been seen in Figs. 4.23 and 4.24. Both heat transfer and inner heat transfer coefficient are increasing with mass flow rate.

4.1.3.3 Study of right side panel

All the results are shown in Table A8 and B8 for both the refrigerants. For this panel results are converging up to .01 kg/s for R134a and 0.006 kg/s for R12. So the results are obtained in the range of 0.001 kg/s to 0.01 kg/s for R134a and 0.001 kg/s to 0.006 kg/s for R12. This is shown in Figs. 4.25 and 4.26.

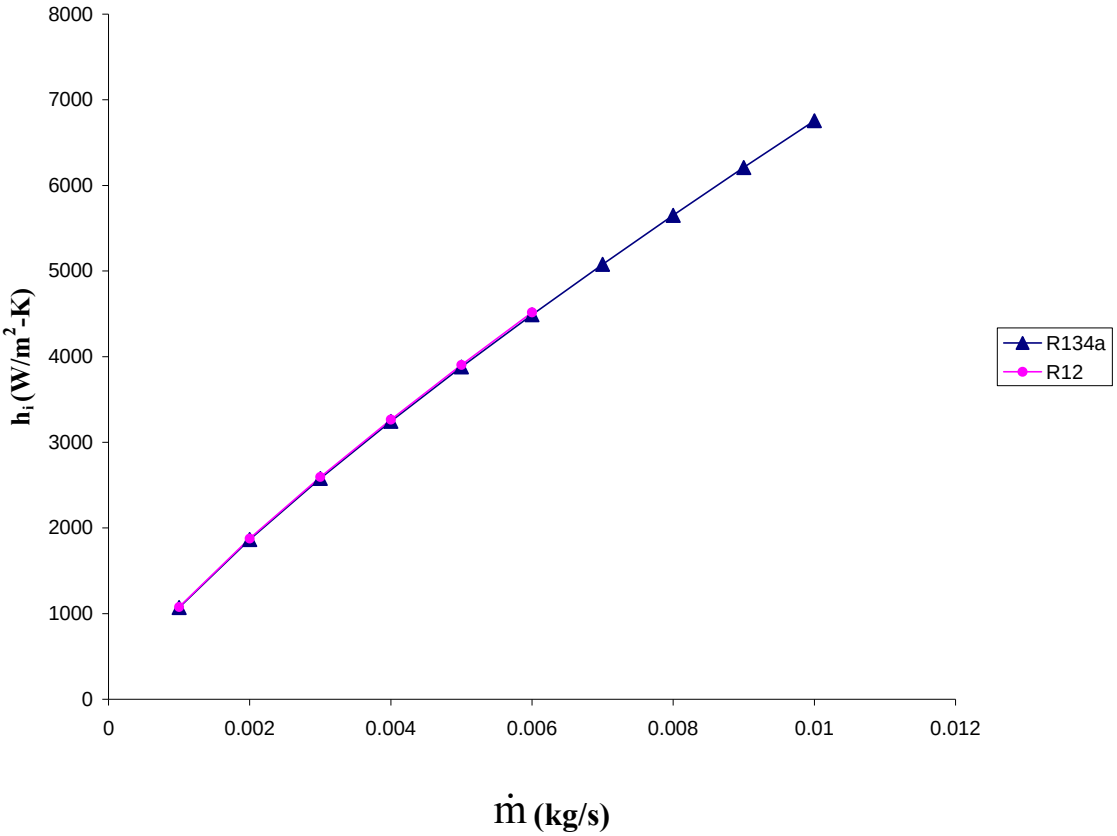

Fig.4.25 Effect of mass flow rate on inner heat transfer coefficient (right side panel)

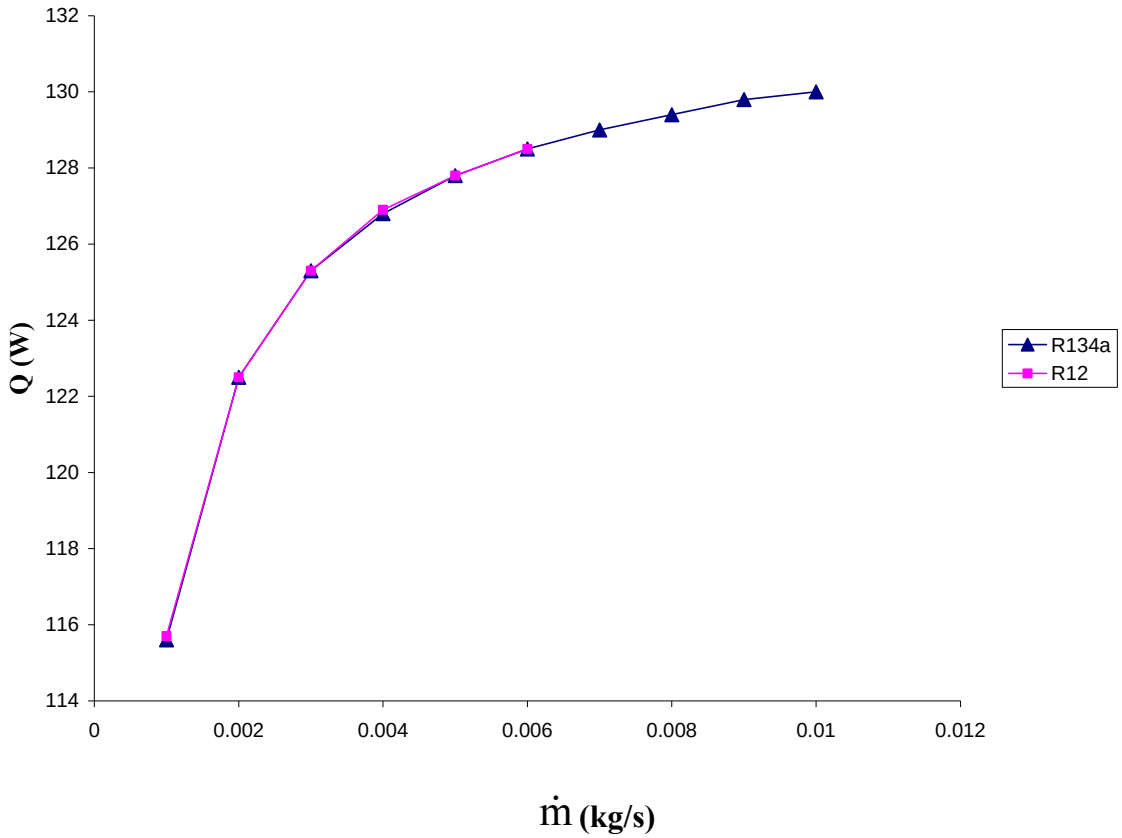

Fig.4.26 Effect of mass flow rate on total heat rejected (up to right side panel)

From Table A8 and B8, it can be concluded that only inner heat transfer coefficient depend upon mass flow rate. The behaviour of inner heat transfer coefficient and heat flow rate has been seen in Figs. 4.25 and 4.26. Both heat transfer and inner heat transfer coefficient are increasing with mass flow rate.

4.1.3.4 Study of cross rail

All the results are shown in Table A9 and B9 for both the refrigerants. For this panel results are converging up to .01 kg/s for R134a and 0.009 kg/s for R12. So the results are obtained in the range of 0.001 kg/s to 0.01 kg/s for R134a and 0.001 kg/s to 0.009 kg/s for R12. This is shown in Figs. 4.27 and 4.28.

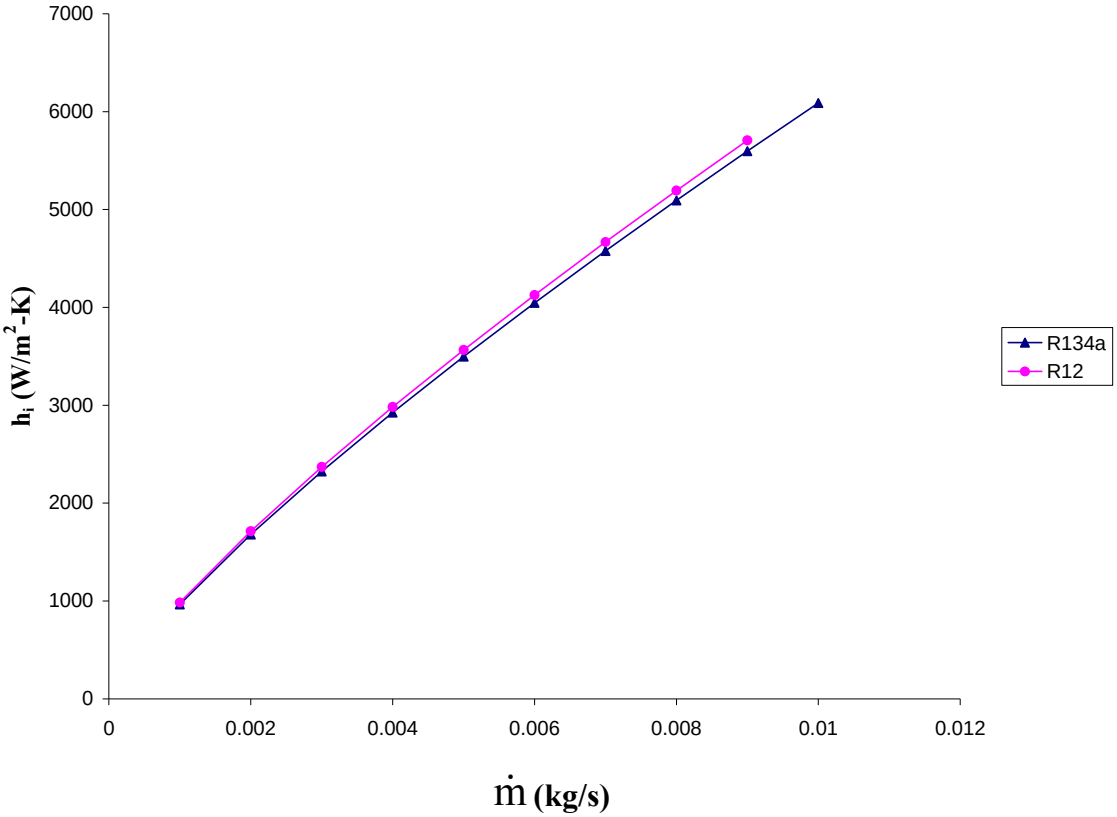

Fig.4.27 Effect of mass flow rate on inner heat transfer coefficient (cross rail)

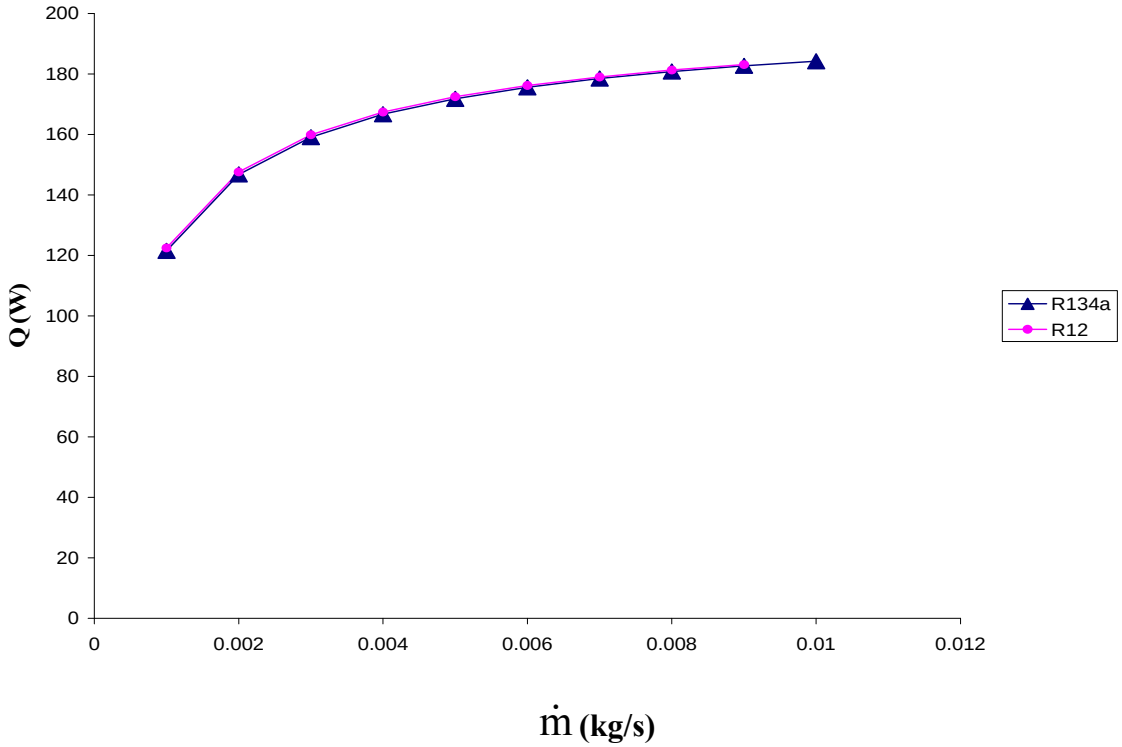

Fig.4.28 Effect of mass flow rate on total heat rejected (up to cross rail)

From Table A9 and B9, it can be concluded that only inner heat transfer coefficient depend upon mass flow rate. The behaviour of inner heat transfer coefficient and heat flow rate has been seen in Figs. 4.27 and 4.28. Both heat transfer and inner heat transfer coefficient are increasing with mass flow rate.

4.1.3.5 Study of left side panel

All the results are shown in Table A10 and B10 for both the refrigerants. For this panel results are converging up to .01 kg/s for R134a and 0.01kg/s for R12. So the results are obtained in the range of 0.001 kg/s to 0.01 kg/s for R134a and 0.001 kg/s to 0.01 kg/s for R12. This is shown in Figs. 4.29 and 4.30.

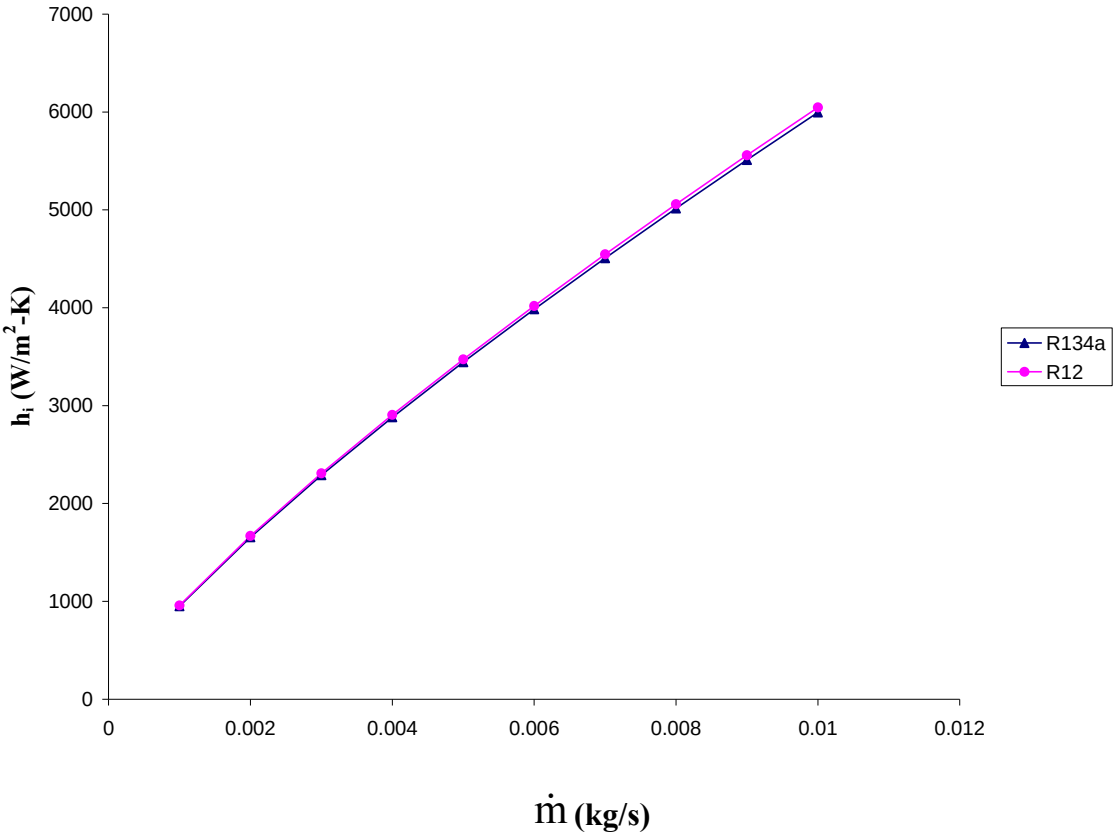

Fig.4.29 Effect of mass flow rate on inner heat transfer coefficient (left side panel)

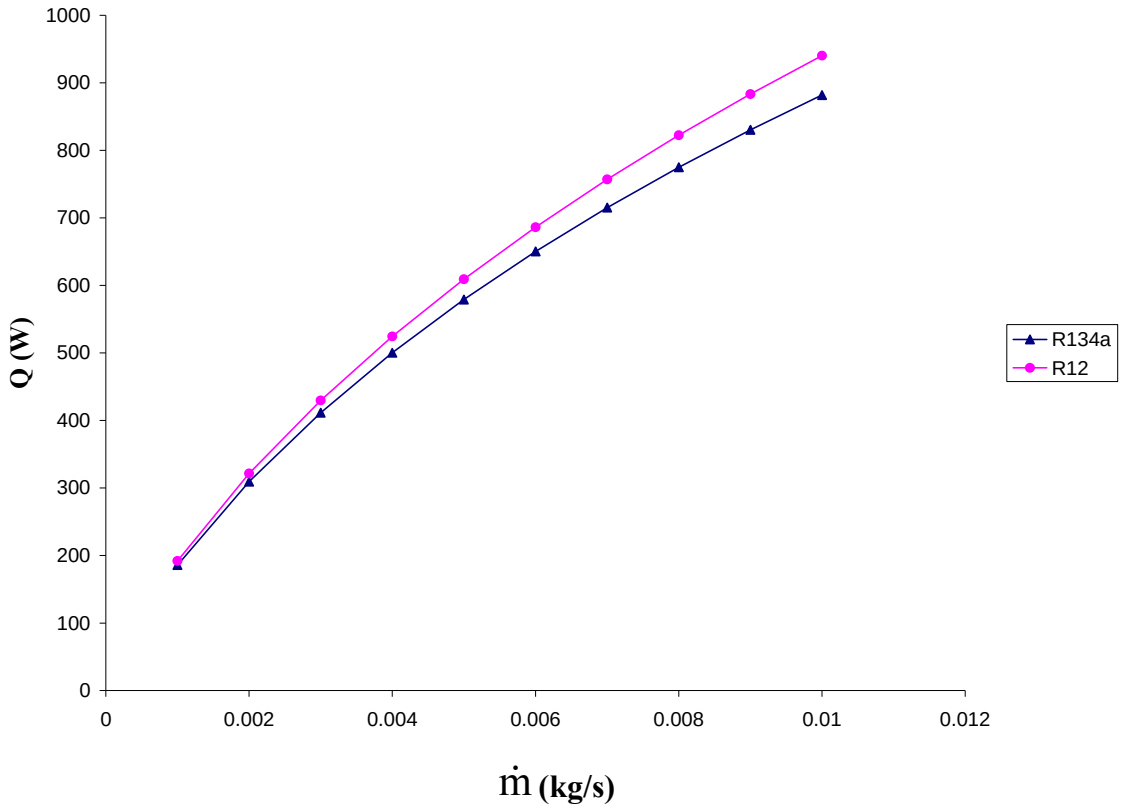

Fig.4.30 Effect of mass flow rate on heat rejected (up to left side panel)

From Table A10 and B10, it can be concluded that only inner heat transfer coefficient depend upon mass flow rate. The behaviour of inner heat transfer coefficient and heat flow rate has been seen in Figs. 4.29 and 4.30. Both heat rejected in condenser and inner heat transfer coefficient are increasing with mass flow rate.

It can be observed that for all the cases inside heat transfer coefficient increases when mass flow rate increases. This is because as the mass flow rate increases, velocity of refrigerant also increases. Because of higher velocity Reynold number also increases, thus Nusselt number increases. So because of increase in Nusselt number, inside heat transfer coefficient increases. Outside heat transfer coefficient remains unaffected due to increase in refrigerant mass flow rate. But, overall heat transfer coefficient increases with mass flow rate. Hence, condenser capacity (Q) increases with mass flow rate.

4.2 Validation of the Results

For the validation purpose comparison of the results of this work with the work done by Bansal and Chin [2002], for the same input conditions that are 40°C refrigerant temperature and 25°C ambient temperature, has been done.

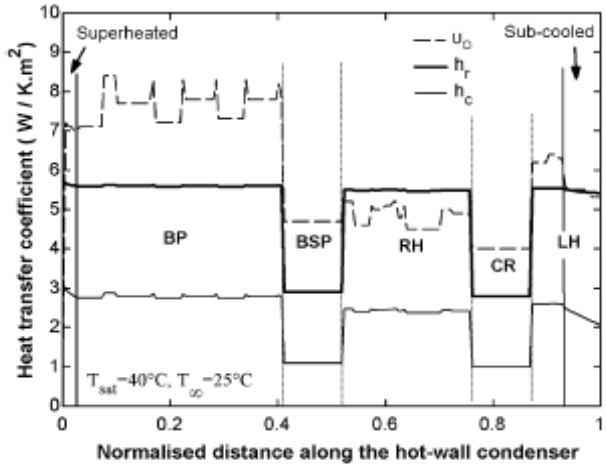

Fig.4.31 Experimental variation of heat transfer coefficients along the condenser, (Bansal and Chin [2002])

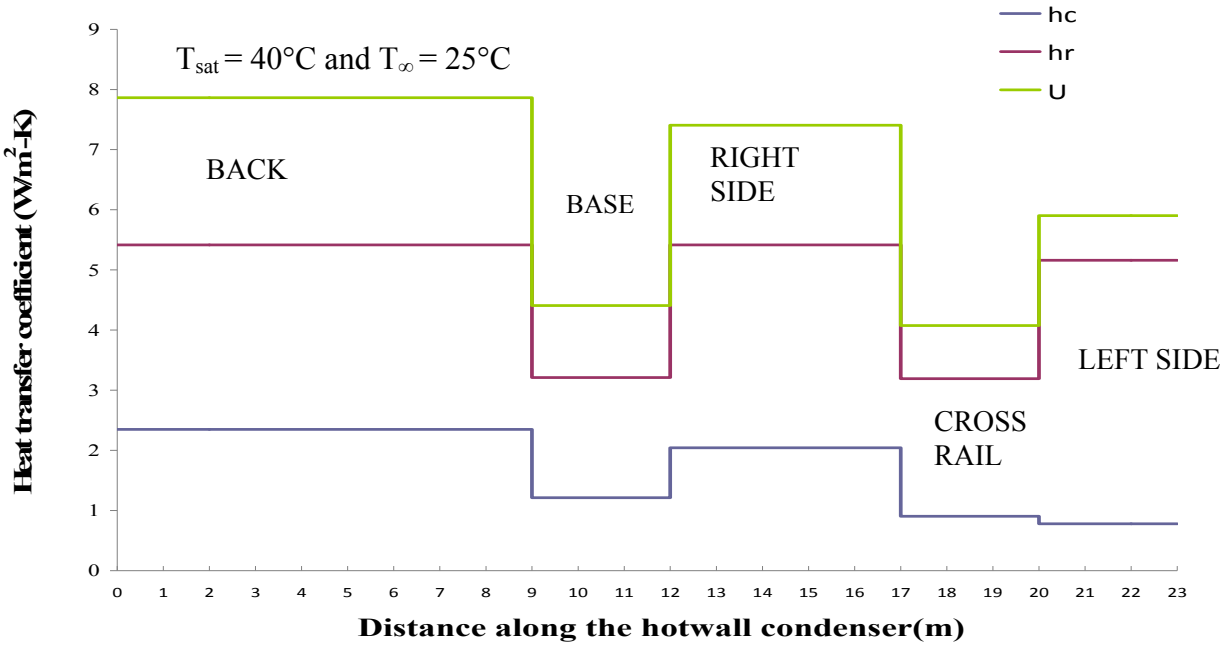

Fig.4.32 Calculated heat transfer coefficients along the condenser

Results obtained by Bansal and Chin [2002] have been shown in Fig. 4.31 and the results of present work have been shown in Fig. 4.32. For the valiation point of view the results of present work are compared with the results of Bansal and Chin [2002] and are shown in Table 4.7.

Table 4.7 Comparison of the results

Parameters	Name of the panel	Bansal and Chin [2002]	Present work
h_c (W/m^2-K)	BACK	2.750	2.347
	BASE	1.115	1.213
	RIGHT SIDE	2.452	2.042
	CROSS RAIL	.9098	.9025
	LEFT SIDE	1.253	.7783
h_r (W/m^2-K)	BACK	5.556	5.545
	BASE	3.310	3.210
	RIGHT SIDE	5.497	5.415
	CROSS RAIL	3.350	3.190
	LEFT SIDE	5.371	5.160
U (W/m^2-K)	BACK	7.775	7.862
	BASE	4.452	4.406
	RIGHT SIDE	6.982	7.405
	CROSS RAIL	4.112	4.075
	LEFT SIDE	5.931	5.902

From Figs. 4.31 and 4.32 and Table 4.7 comparision can be done easily.1 to 2 % variation is found in the case of convective and radiative heat transfer coefficients. More varition is found in the case of overall heat transffer coefficient which is because the contact resistance has been neglected in the calulation in the present work.

As shown in Table 4.7 the results obtained in this study show an excellent agreement with the results reported by Bansal and Chin [2002].

4.3 Comparison of R134a and R12 condenser

After getting all the simulation results for both the refrigerants, comparison can be done based on different parameters such as panel wise drop in dryness fraction, heat transfer coefficients and pressure drop. The comparison of the two refrigerant condensers has been made for mass flow rate of 0.001 kg/s, ambient temperature of 25ºC and condenser temperature of 40 ºC.

4.3.1 Comparison based on decrease in dryness fraction

From the Fig. 4.33**,** it can be seen that faster quality drop occurs in case of R12 refrigerant. From the results, quality at the end of condensation is found to be subcooled in the case of R12 whereas in the case of R134a it is obtained as nearly saturated (x = 0.0083).

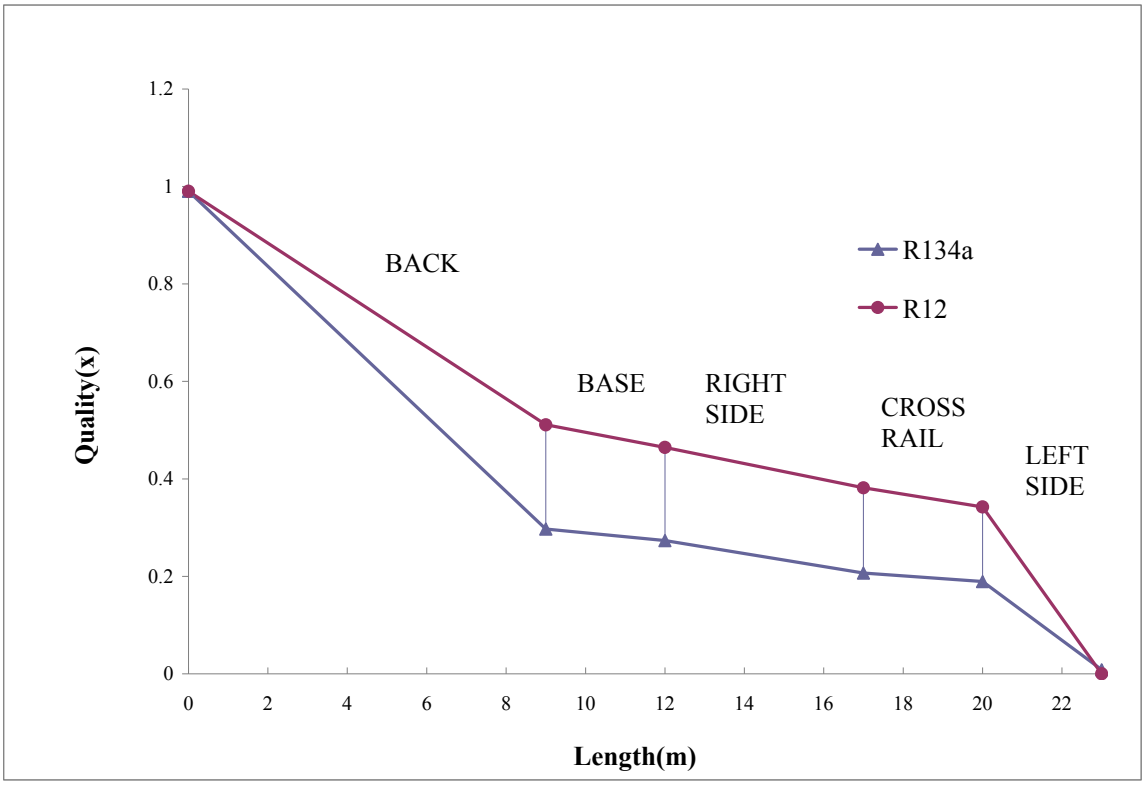

Fig.4.33 Change in quality (x) with length of condenser

4.3.2 Comparison based on outside heat transfer coefficient

As far as outside heat transfer coefficient is concerned, the difference is insignificant. Radiative heat transfer coefficients for the two refrigerants have almost same value, whereas in case of convective heat transfer coefficient the difference is negligible. This is evident from Fig. 4.34 to 4.36.

The reason of this behaviour is that on outside, air is the fluid in both the cases and variation in average plate temperature is very small for the two refrigerants.

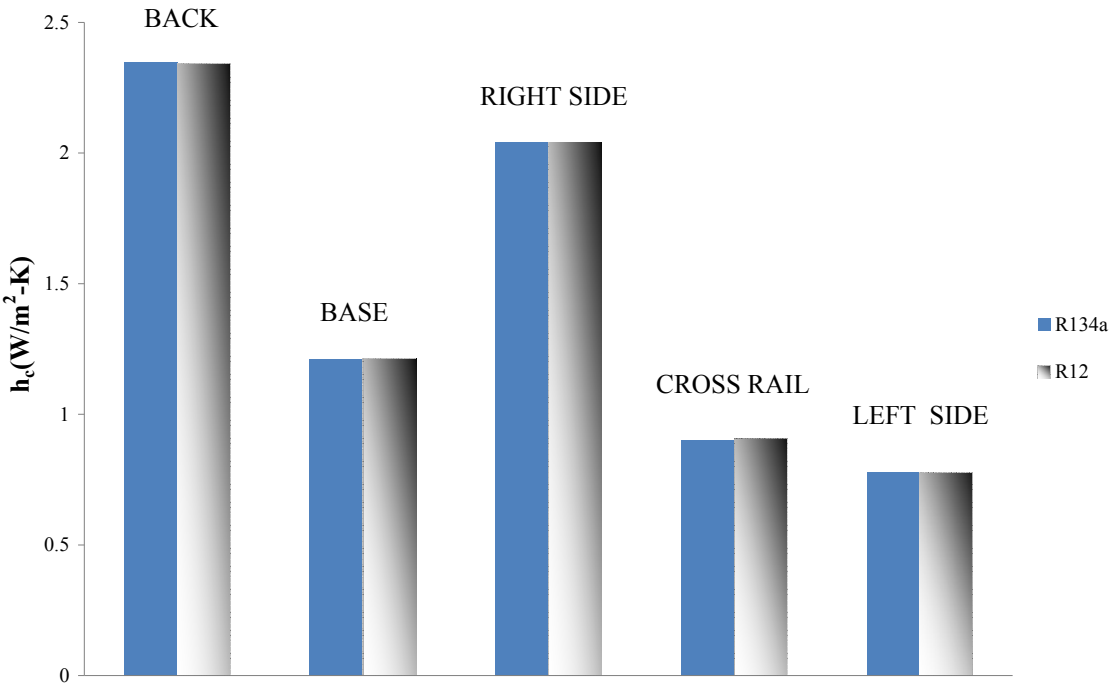

Fig.4.34 Comparison based on convective heat transfer coefficient (panel wise)

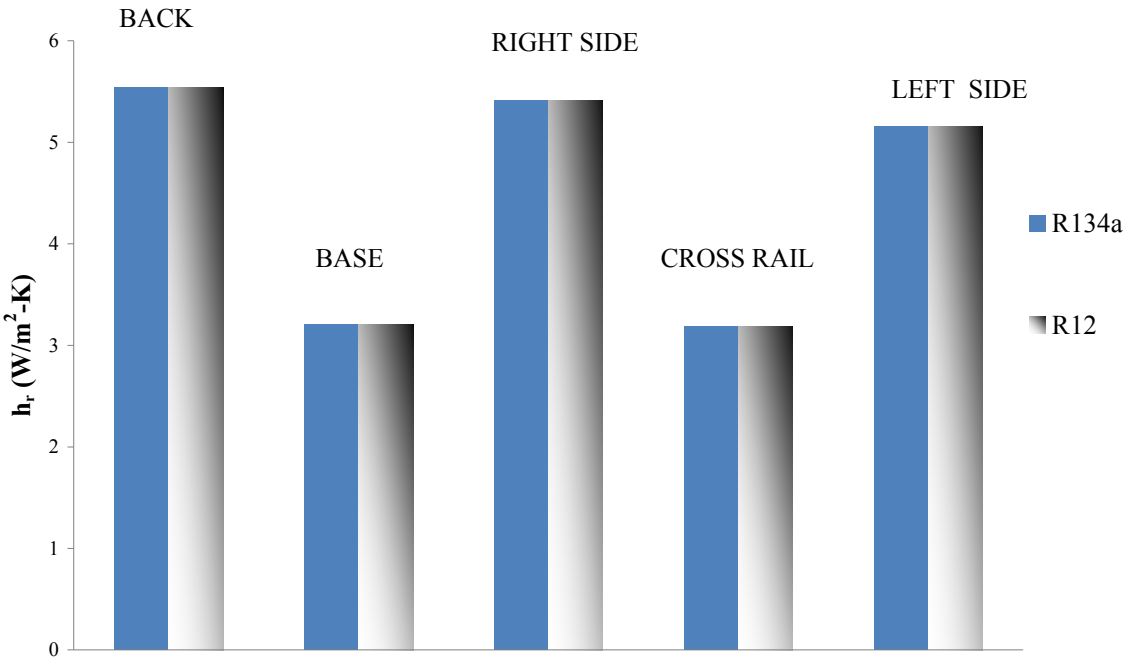

Fig.4.35 Comparison based on the radiative heat transfer coefficient (panel wise)

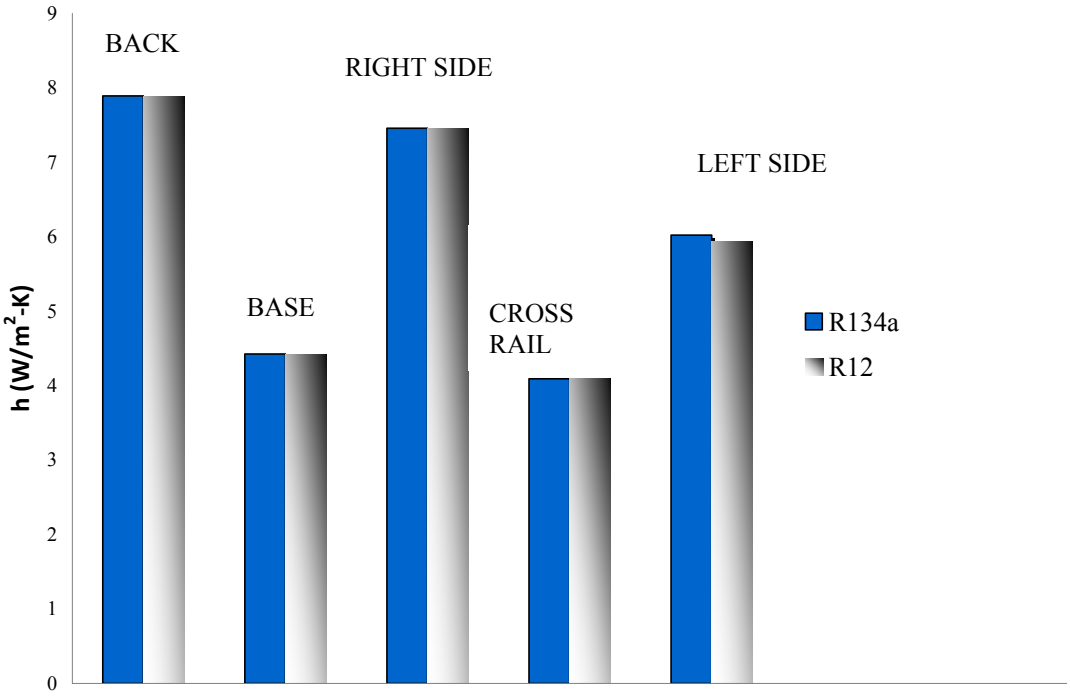

Fig.4.36 Comparison based on the total outer heat transfer coefficient (panel wise)

4.3.3 Comparison based on inner heat transfer coefficient

By simulation results, it can be seen that inner heat transfer coefficient is lower for R134a except in the back panel. Among all the cases for R134a inner heat transfer coefficient has highest value for back panel. That is why maximum quality drop is found in the back panel. This also means that most of the condensation occurs in the back panel. The comparison for R134a and R12 has been shown in Fig. 4.37.

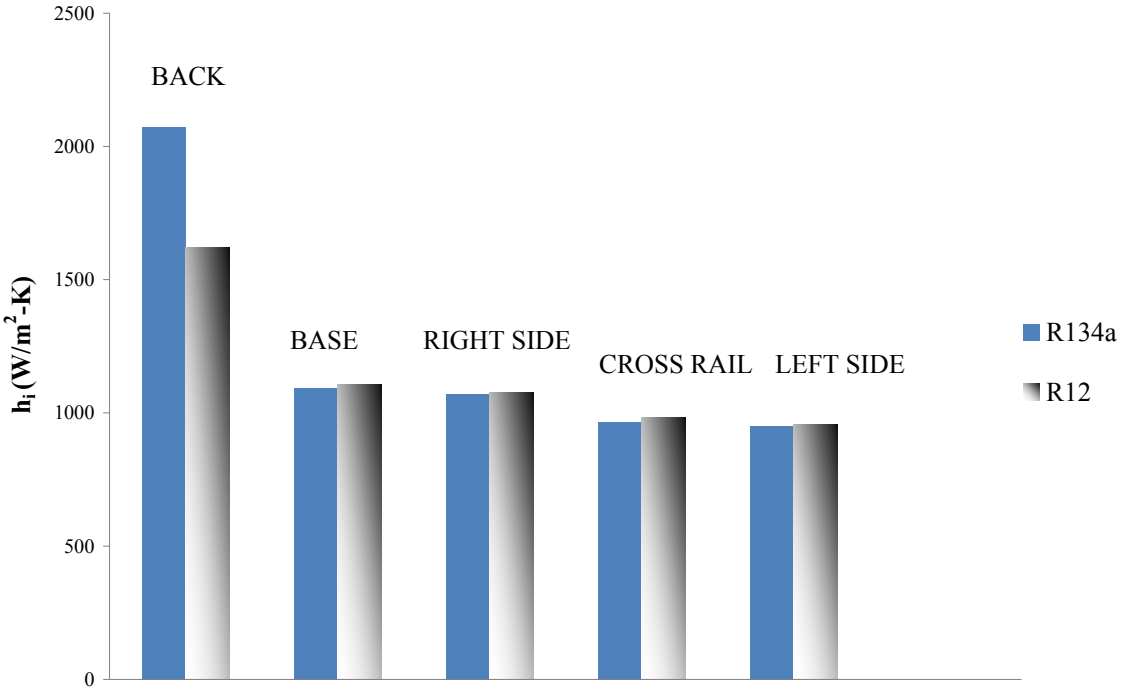

Fig.4.37 Comparison based on the inner heat transfer coefficient (panel wise)

4.3.4. Comparison based on pressure drop

From the simulation results, it can be seen that pressure drop is more in the back panel for both the refrigerants. Except in the back panel, the pressure drop is very small in all other panels for both the refrigerants. This is because of higher velocity of refrigerant in the back panel and as condensation starts, velocity of refrigerants decreases due to phase transformation. The pressure drop in all the panels for both the refrigerants is given in Table 4.8.

Table 4.8 Comparison of preessure drop for both refrigerants

Refrigerant	Name of the panel	Pressure drop(kPa)	Total pressure drop in condenser (kPa)
R134a	BACK	116.8	132.700
	BASE	2.600	
	RIGHT SIDE	6.300	
	CROSS RAIL	3.000	
	LEFT SIDE	4.000	
R12	BACK	108.4	120.506
	BASE	1.906	
	RIGHT SIDE	4.828	
	CROSS RAIL	2.371	
	LEFT SIDE	3.001	

From Table 4.8, it can be seen that total pressure drop in the condenser using R134a is little higher (10.1 %) compared to that for R12.

Chapter 5

CONCLUSIONS

A simulation model for the hot wall condenser has been developed and results of simulation have been presented in this report for refrigerant R134a and R12. The simulation is quite unique, because it has been written in EES, which is quiet easy to understand. The heat transfer parameters studied in this work are; convective and radiative heat transfer coefficients on outer side of the tube and convective heat transfer coefficient on the inner side of the tube. Apart from these parameters, pressure drop in the condenser has also been calculated. The effect of operating parameters such as ambient temperature and mass flow rate of the refrigerant on various heat transfer coefficients has been studied. The effect of operating parameters on condenser heat load has also been studied.

From the results, it can be concluded that the performance of the refrigerator marginally goes down due to replacement of R12 with R134a, however it can be understood that this small decline in the performance is justifiable due to ozone friendly nature of R134a and ban on the use of R12.

The results of the simulation can be summarized in brief as follows:

1. For the giving length of the condenser, subcooled liquid is found at the outlet of condenser in case of R12 whereas it is saturated liquid in case of R134a.
2. The inside heat transfer coefficient is marginally lower for R134a compared to that for R12 where as outside heat transfer coefficient is found to be almost same for both the refrigerants.
3. For the given design conditions ($\dot{m} = 0.001$ kg/s, $T_{ambient} = 25$ºC and $T_{condenser} = 40$ ºC), the pressure drop in case of R134a is found to 132.7 kPa whereas it is 120.5 kPa for R12.

REFERENCES

[1]. Bansal P.K., Chin T.C., Design and modelling of hot-wall condensers in domestic refrigerators, International Journal of Applied Thermal Engineering ,2002,22, 1601–1617.

[2]. Bansal P.K., Chin T.C., Modelling and optimisation of the wire-and-tube condensers, International Journal of Refrigeration, 2003,26,601–613.

[3]. Breber G., Palen J.W., Taborek J., Prediction of horizontal tube side condensation of pure components using flow regime criteria, Journal of Heat Transfer ,1980,102, 471–476.

[4]. Cavillini A., Zecchin R., High velocity condensation of R-11 vapors inside vertical tubes. Heat transfer in refrigeration, International Institute of Refrigeration,1971, 385–396.

[5]. Engineering Equation Solver, Demo version, 1992-2006.

[6]. Incropera F.P., Witt D.P. De, Fundamentals of Heat and Mass Transfer, third ed., John Wiley & Sons, Inc, NewYork, 1990.

[7]. Jaster H., Kosky P.G., Condensation heat transfer in a mixed flow regime, International Journal of Heat and Mass Transfer ,1976,19, 95–99.

[8]. Kakac S., Liu H., Heat Exchangers Selection, Rating, and Thermal Design, CRC Press, New York, 1998.

[9]. Kothadaraman C.P., Subramanyam S, Heat and mass transfer data book, fifth edition,2004, New age publication.

[10]. Martinelli R.C., Lockhart R.W., Proposed correlation data for isothermal two phase, two-component flow in pipes, Chemical Engineering Proceeding,1949,45, 39–48.

[11]. Mills A.F., Basic Heat and Mass Transfer, second ed., Prentice Hall, Upper addler River, NJ, 1999.

[12]. Mueller A.C., Heat Exchanger Design Handbook, Hemisphere Publishing Corporation, New York, 1983, Section 3.4.6.

[13]. Radermacher R. and Kim K., Domestic refrigerators: recent developments, review paper, 1996, 19, 61-69.

[14]. Rousseau P.G., Eldik M. van, Greyvenstein G.P., Detailed simulation of fluted tube water heating condensers, International Journal of Refrigeration, 2003,26, 232–239.

[15]. Tagliafico L., Tanda G., Radiation and natural convection heat transfer from wire-and-tube heat exchangers in refrigeration appliances, International Journal of Refrigeration 1997,20(7), 461–469.

[16]. Thome John R., Engineering data book iii, chapter 17, first edition, 2004.

[17]. Whalley P.B., Boiling, Condensation and Gas- liquid flow, Clarendon press, Oxford Engineering Science Series 21, 1987.

APPENDIX A

Tables for R134a

Appendix A.1 In this section tables, showing effect of ambient temperature on heat transfer parameters in all the panels, are given. Heat rejected, ($\sum Q$) given in all the tables is the total heat rejected up to that panel for which table is given.

Table A1 Effect of ambient temperature on heat transfer parameters in back panel

Input condition: mass flow rate 0.001 kg/s

T_∞ (K)	h_c (W/m^2-K)	h_r (W/m^2-K)	h (W/m^2-K)	h_i (W/m^2-K)	$\sum Q$ (W)
312	1.057	5.934	6.991	2074	6.677
309	1.649	5.848	7.498	2074	26.71
305	1.989	5.736	7.725	2074	53.42
301	2.214	5.626	7.840	2074	80.13
297	2.387	5.518	7.906	2074	106.80
293	2.531	5.412	7.944	2074	133.50

Table A2 Effect of ambient temperature on heat transfer parameters in base panel

Input condition: mass flow rate 0.001 kg/s

T_∞ (K)	h_c (W/m^2-K)	h_r (W/m^2-K)	h (W/m^2-K)	h_i (W/m^2-K)	$\sum Q$ (W)
309	0.5239	3.547	4.071	1092	27.45
305	0.9516	3.422	4.374	1092	55.83
301	1.121	3.3	4.421	1092	85.22
297	1.24	3.181	4.421	1092	114.6
293	1.334	3.064	4.399	1092	144

Table A3 Effect of ambient temperature on heat transfer parameters in right side panel

Input condition: mass flow rate 0.001 kg/s

T_∞ (K)	h_c (W/m^2-K)	h_r (W/m^2-K)	h (W/m^2-K)	h_i (W/m^2-K)	$\sum Q$ (W)
307	1.121	5.661	6.782	1071	24.34
305	1.500	5.606	7.106	1071	64.62
301	1.864	5.496	7.36	1071	90.18
297	2.092	5.388	7.48	1071	125.7
296	2.139	5.362	7.501	1071	135.9

Table A4 Effect of ambient temperature on heat transfer parameters in cross rail

Input condition: mass flow rate 0.001 kg/s

T_∞ (K)	h_c (W/m^2-K)	h_r (W/m^2-K)	h (W/m^2-K)	h_i (W/m^2-K)	$\sum Q$ (W)
303	0.5515	3.345	3.896	964.9	80.12
301	0.7524	3.282	4.035	964.9	94.67
299	0.8608	3.22	4.081	964.9	109.2
297	0.9393	3.159	4.099	964.9	133.7
296	0.9723	3.129	4.101	964.9	146

Table A5 Effect of ambient temperature on heat transfer parameters in left side panel

Input condition: mass flow rate 0.001 kg/s

T_∞ (K)	h_c (W/m^2-K)	h_r (W/m^2-K)	h (W/m^2-K)	h_i (W/m^2-K)	$\sum Q$ (W)
298.1	0.6551	5.163	5.818	950.3	182.6
298.0	0.777	5.16	5.937	950.3	185.8

Appendix A.2 In this section all the tables, showing effect of mass flow rate on heat transfer parameters in all the panels, are given. Heat rejected, (Q) given in all the tables is the total heat rejected up to that panel for which table is given.

Table A6 Effect of mass flow rate on heat transfer parameters in back panel

Input condition: ambient temperature 25°C

$\dot{m}$ (kg/s)	h_c (W/m^2-K)	h_r (W/m^2-K)	h (W/m^2-K)	h_i (W/m^2-K)	$\sum Q$ (W)
0.001	2.347	5.545	7.892	2074	100.2
0.002	2.347	5.545	7.892	3612	100.3
0.003	2.347	5.545	7.892	4996	101.7
0.004	2.347	5.545	7.892	6289	102.0
0.005	2.347	5.545	7.892	7518	102.1
0.006	2.347	5.545	7.892	8698	102.2
0.007	2.347	5.545	7.892	9840	102.3
0.008	2.347	5.545	7.892	10949	102.4
0.009	2.347	5.545	7.892	12031	102.4
0.01	2.347	5.545	7.892	13089	102.4

Table A7 Effect of mass flow rate on heat transfer parameters in base panel

Input condition: ambient temperature 25°C

$\dot{m}$ (kg/s)	h_c (W/m^2-K)	h_r (W/m^2-K)	h (W/m^2-K)	h_i (W/m^2-K)	$\sum Q$ (W)
0.001	1.213	3.21	4.424	1092	107.3
0.002	1.213	3.21	4.424	1901	118
0.003	1.213	3.21	4.424	2629	122.6
0.004	1.213	3.21	4.424	3309	125.2
0.005	1.213	3.21	4.424	3956	126.9
0.006	1.213	3.21	4.424	4577	128.2
0.007	1.213	3.21	4.424	5178	129.1
0.008	1.213	3.21	4.424	5761	129.8
0.009	1.213	3.21	4.424	6331	130.4
0.01	1.213	3.21	4.424	6887	130.8

Table A8 Effect of mass flow rate on heat transfer parameters in right side panel

Input condition: ambient temperature 25°C

$\dot{m}$ (kg/s)	h_c (W/m^2-K)	h_r (W/m^2-K)	h (W/m^2-K)	h_i (W/m^2-K)	$\sum Q$ (W)
0.001	2.042	5.415	7.457	1071	115.6
0.002	2.042	5.415	7.457	1864	122.5
0.003	2.042	5.415	7.457	2578	125.3
0.004	2.042	5.415	7.457	3245	126.8
0.005	2.042	5.415	7.457	3880	127.8
0.006	2.042	5.415	7.457	4489	130.5
0.007	2.042	5.415	7.457	5078	131.0
0.008	2.042	5.415	7.457	5651	133..4
0.009	2.042	5.415	7.457	6209	135.8
0.01	2.042	5.415	7.457	6755	140.0

Table A9 Effect of mass flow rate on heat transfer parameters in cross rail

Input condition: ambient temperature 25°C

$\dot{m}$ (kg/s)	h_c (W/m^2-K)	h_r (W/m^2-K)	h (W/m^2-K)	h_i (W/m^2-K)	$\sum Q$ (W)
0.001	0.9025	3.19	4.092	964.9	121.5
0.002	0.9025	3.19	4.092	1680.0	146.8
0.003	0.9025	3.19	4.092	2324	159.1
0.004	0.9025	3.19	4.092	2925	166.7
0.005	0.9025	3.19	4.092	3497	171.8
0.006	0.9025	3.19	4.092	4046	175.6
0.007	0.9025	3.19	4.092	4577	178.5
0.008	0.9025	3.19	4.092	5093	180.8
0.009	0.9025	3.19	4.092	5596	182.7
0.01	0.9025	3.19	4.092	6088	184.2

Table A10 Effect of mass flow rate on heat transfer parameters in left side panel

Input condition: ambient temperature 25°C

$\dot{m}$ (kg/s)	h_c (W/m^2-K)	h_r (W/m^2-K)	h (W/m^2-K)	h_i (W/m^2-K)	$\sum Q$ (W)
0.001	0.777	5.16	5.937	950.3	185.8
0.002	0.777	5.16	5.937	1654	309.3
0.003	0.777	5.16	5.937	2288	411.5
0.004	0.777	5.16	5.937	2881	500.2
0.005	0.777	5.16	5.937	3444	579.1
0.006	0.777	5.16	5.937	3984	650.3
0.007	0.777	5.16	5.937	4507	715.2
0.008	0.777	5.16	5.937	5015	775.0
0.009	0.777	5.16	5.937	5511	830.4
0.01	0.777	5.16	5.937	5996	831.9

APPENDIX B

Tables for R12

Appendix B.1 In this section all the tables, showing effect of ambient temperature on heat transfer parameters in all the panels, are given. Heat rejected, (Q) given in all the tables is the total heat rejected up to that panel for which table is given.

Table B1 Effect of ambient temperature on heat transfer parameters in back panel

Input condition: mass flow rate 0.001 kg/s

T_∞ (K)	h_c (W/m^2-K)	h_r (W/m^2-K)	h (W/m^2-K)	h_i (W/m^2-K)	$\sum Q$ (W)
308	1.744	5.817	7.561	1623	33.11
306	1.912	5.761	7.674	1623	45.36
304	2.046	5.706	7.752	1623	59.60
302	2.158	5.651	7.809	1623	72.85
300	2.256	5.596	7.853	1623	86.09
298	2.343	5.542	7.885	1623	99.34
296	2.422	5.489	7.911	1623	112.6
294	2.494	5.436	7.930	1623	125.8
292	2.561	5.383	7.944	1623	139.1
290	2.624	5.331	7.955	1623	152.3

Table B2 Effect of ambient temperature on heat transfer parameters in base panel

Input condition: mass flow rate 0.001 kg/s

T_∞ (K)	h_c (W/m^2-K)	h_r (W/m^2-K)	h (W/m^2-K)	h_i (W/m^2-K)	$\sum Q$ (W)
309	0.5239	3.547	4.071	1109	25.80
307	0.8173	3.484	4.302	1109	40.54
305	0.8516	3.422	4.374	1109	55.28
303	1.0460	3.361	4.407	1109	70.03
301	1.2100	3.300	4.421	1109	84.77
299	1.1850	3.240	4.425	1109	99.51
297	1.2400	3.181	4.421	1109	114.30
295	1.2900	3.122	4.412	1109	129.00
293	1.3340	3.064	4.399	1109	143.70
291	1.3760	3.007	4.383	1109	158.50

Table B3 Effect of ambient temperature on heat transfer parameters in right side panel

Input condition: mass flow rate 0.001 kg/s

T_∞ (K)	h_c (W/m^2-K)	h_r (W/m^2-K)	h (W/m^2-K)	h_i (W/m^2-K)	$\sum Q$ (W)
307	1.121	5.661	6.782	1077	44.36
305	1.500	5.606	7.106	1077	60.65
303	1.710	5.551	7.261	1077	74.95
301	1.864	5.496	7.360	1077	85.25
299	1.987	5.442	7.429	1077	105.50
297	2.092	5.388	7.480	1077	125.80
295	2.184	5.335	7.519	1077	146.10
293	2.266	5.282	7.548	1077	166.40
291	2.340	5.23	7.570	1077	186.70
289	2.408	5.178	7.587	1077	207.00

Table B4 Effect of ambient temperature on heat transfer parameters in cross rail

Input condition: mass flow rate 0.001 kg/s

T_∞ (K)	h_c (W/m^2-K)	h_r (W/m^2-K)	h (W/m^2-K)	h_i (W/m^2-K)	$\sum Q$ (W)
303	0.5677	3.345	3.913	984.1	80.82
302	0.6832	3.314	3.997	984.1	83.00
301	0.7589	3.282	4.041	984.1	88.37
300	0.8171	3.251	4.068	984.1	97.74
299	0.8651	3.221	4.086	984.1	110.10
298	0.9063	3.190	4.096	984.1	122.50
297	0.9426	3.159	4.102	984.1	134.90
296	0.9753	3.129	4.104	984.1	147.20
295	1.0050	3.099	4.104	984.1	159.60
294	1.0320	3.069	4.102	984.1	172

Table B5 Effect of ambient temperature on heat transfer parameters in left side panel

Input condition: mass flow rate 0.001 kg/s

T_∞ (K)	h_c (W/m^2-K)	h_r (W/m^2-K)	h (W/m^2-K)	h_i (W/m^2-K)	$\sum Q$ (W)
298	0.778	5.160	5.939	958.30	192.1
297	1.213	5.134	6.347	958.30	224.7
296	1.410	5.108	6.518	958.30	257.3
295	1548	5.082	6.631	958.30	289.8
294	1.657	5.056	6.714	958.30	322.4
293	1.748	5.031	6.779	958.30	355.0
292	1.827	5.005	6.832	958.30	387.5
291	1.898	4.980	6.877	958.30	420.1
290	1.961	4.950	6.915	958.30	452.7
289	2.019	4.929	6.948	958.30	485.2

Appendix B.2 In this section all the tables, showing effect of mass flow rate on heat transfer parameters in all the panels, are given. Heat rejected, (Q) given in all the tables is the total heat rejected up to that panel for which table is given.

Table B6 Effect of mass flow rate on heat transfer parameters in back panel

Input condition: ambient temperature 25°C

$\dot{m}$ (kg/s)	h_c (W/m^2-K)	h_r (W/m^2-K)	h (W/m^2-K)	h_i (W/m^2-K)	$\sum Q$ (W)
0.001	2.343	5.542	7.885	1623	99.34
0.002	2.343	5.542	7.885	2827	100.80
0.003	2.343	5.542	7.885	3910	101.30
0.004	2.343	5.542	7.885	4921	101.60

Table B7 Effect of mass flow rate on heat transfer parameters in base panel

Input condition: ambient temperature 25°C

$\dot{m}$ (kg/s)	h_c (W/m^2-K)	h_r (W/m^2-K)	h (W/m^2-K)	h_i (W/m^2-K)	$\sum Q$ (W)
0.001	1.213	3.21	4.424	1109	106.9
0.002	1.213	3.21	4.424	1931	117.5
0.003	1.213	3.21	4.424	2671	122.0
0.004	1.213	3.21	4.424	3362	124.5
0.005	1.213	3.21	4.424	4019	126.2

Table B8 Effect of mass flow rate on heat transfer parameters in right side panel

Input condition: ambient temperature 25°C

$\dot{m}$ (kg/s)	h_c (W/m^2-K)	h_r (W/m^2-K)	h (W/m^2-K)	h_i (W/m^2-K)	$\sum Q$ (W)
0.001	2.042	5.415	7.457	1077	115.7
0.002	2.042	5.415	7.457	1876	122.5
0.003	2.042	5.415	7.457	2595	125.3
0.004	2.042	5.415	7.457	3266	126.9
0.005	2.042	5.415	7.457	3904	127.8
0.006	2.042	5.415	7.457	4517	128.5

Table B9 Effect of mass flow rate on heat transfer parameters in cross rail

Input condition: ambient temperature 25°C

$\dot{m}$ (kg/s)	h_c (W/m^2-K)	h_r (W/m^2-K)	h (W/m^2-K)	h_i (W/m^2-K)	$\sum Q$ (W)
0.001	0.9063	3.19	4.096	984	122.5
0.002	0.9063	3.19	4.096	1713	147.6
0.003	0.9063	3.19	4.096	2370	159.9
0.004	0.9063	3.19	4.096	2983	167.4
0.005	0.9063	3.19	4.096	3566	172.5
0.006	0.9063	3.19	4.096	4126	176.2
0.007	0.9063	3.19	4.096	4668	179.0
0.008	0.9063	3.19	4.096	5194	181.3
0.009	0.9063	3.19	4.096	5707	183.1

Table B10 Effect of mass flow rate on heat transfer parameters in left side panel

Input condition: ambient temperature 25°C

$\dot{m}$ (kg/s)	h_c (W/m^2-K)	h_r (W/m^2-K)	h (W/m^2-K)	h_i (W/m^2-K)	$\sum Q$ (W)
0.001	.7783	5.16	5.939	958	192.1
0.002	.7783	5.16	5.939	1669	321.5
0.003	.7783	5.16	5.939	2308	429.7
0.004	.7783	5.16	5.939	2905	524.4
0.005	.7783	5.16	5.939	3473	609.2
0.006	.7783	5.16	5.939	4018	686.2
0.007	.7783	5.16	5.939	4546	757.0
0.008	.7783	5.16	5.939	5058	822.4
0.009	.7783	5.16	5.939	5558	883.3
0.01	.7783	5.16	5.939	6047	940.3

APPENDIX C

This section includes a sample program for the simulation of back panel which is written in equation window of Engineering Equation Solver (EES). Results obtained by this simulation program are also given in this section.

```
{" simulation of hotwall condenser"}

"calculation for back panel"

"input for refrigerant at back panel"
T_ref=313[K] ;                          "temperature of refrigerant"
p_ref=1012.5[kPa] ;                     "pressure of refrigerant"
m_dot=.001 [kg/sec] ;                   "mass flow rate of refrigerants"
T_infinity=298[K] ;                     "ambient temperature"

"geometrical data of condenser "

"tube material is stainless steel coated with copper"
d_t_o=.00475[m];                        "tube outer diameter"
d_t_i=.004[m];                          "tube inner diameter"
A_b_p=.8736[m^2];                       "area of back panel"
l_t_b=9.64[m];                          "length of tube in back panel"
A_c=.00001256 [m^2];                    "cross sectional area of tube"
h_b_p=1.4[m];                           "height of the back panel"

"find average width for panel"
w_av_b=A_b_p/l_t_b;                     "average width of back panel"

"set an initial guess value"
h_0=7.892[w/m^2-K] ;                    "outer heat transfer coefficient"
T_0=312.6[k];                           "tube outer temperature"

"find the values for the refrigerant R134a"
T_av=T_ref+(T_0-T_ref)/2;
x=.999;                                 "dryness fraction at inlet of back panel"
h_ref=417.73[kJ/kg];                    "enthalpy at inlet of back panel"
mu_v=.0000123[kg/m-s];                  "vapour viscosity at inlet"
mu_l=.000161[kg/m-s];                   "liquid viscosity at inlet"
rho_i=50.354[kg/m^3];                   "bulk density at inlet"
rho_l=1147.4[kg/m^3];                   "liquid density at inlet"
rho_v=49.872[kg/m^3];                   "vapour density at inlet"
c_p_l=1497[J/kg-K];                     "liquid specific heat at inlet"
c_p_v=1143[J/kg-K];                     "vapor specific heat at inlet"
k_v=.0154[W/m-K];                       "vapour thermal conductivity at inlet"
```

```
k_l=.0747[W/m-K];                    "liquid thermal conductivity at inlet"

"properties of material"
k_f=k_('Stainless_AISI302', T_0)          "thermal conductivity of plate"

"take"
z=8.93[m];                           "elemental length for analysis"

"calculation for efficiency of plate"
m=sqrt((h_0*z)/(k_f*A_b_p)) ;              "fin property parameter"
eta_plate=(tanh(m*w_av_b/2)/(m*w_av_b/2));   "calculate plate efficiency"

"calculation for average temperature of plate"
T_pl_av=eta_plate*(T_0-T_infinity)+T_infinity ;  "average temperature of plate"
epcilen=.859;                                "emisivity of plate"
h_r=epcilen*sigma#*((T_pl_av^4-T_infinity^4)/(T_pl_av-T_infinity));

"compute air properties"
T_a=(T_ref+T_infinity)/2;          "temperature at which air properties will calculated"
rho_a=Density(Air,T=T_a,P=101.325);          "density"
cp_a=Cp(Air,T=T_a)*convert(kJ/kg-K,J/kg-k);   "specific heat"
mu_a=Viscosity(Air,T=T_a);                   "viscosity"
k_a=Conductivity(Air,T=T_a);                 "thermal conductivity"
alpha_a=k_a/(rho_a*cp_a);                    "thermal diffusivity"
Pr_a=Prandtl(Air,T=T_a);                     "prandlt number"
beta_a=1/T_a;                                "temprature coeffecient"

"calculation of Rayleigh number"
L_cha=h_b_p;                                 "characteristic length"
Ra=g#*beta_a*((T_pl_av)-T_infinity)*L_cha^3*rho_a/(mu_a*alpha_a); "Rayleigh
number"

"calculation of nusselt number"
Nus =.68+.67*Ra^.25*(1+(.492/Pr_a)^(9/16))^(-4/9);    "nusselt number"

"calculation of convective heat transfer coefficient"
h_c=Nus*k_a/L_cha;

"convergence"
h=h_c+h_r ;

"computation of equivalent outer heat transfer using parallel heat flow mechanism"
L=w_av_b/2;                                  "length"
R_pl=1/(sqrt(h_0*z*k_f*A_c)*tanh(m*L));      " plate resistance"
R_o_eq=R_pl/2;                       "equivalent resistance for whole plat surface"
```

```
"calculation for internal heat transfer coeffecient"
A_i=pi*d_t_i^2/4;                                   "cross sectional area"
G=m_dot/A_i;                                        "mass flux"
Re_v=G*x*d_t_i/mu_v;                                "vapour reynold number"
Re_l=G*(1-x)*d_t_i/mu_l;                            "liquid reynold number"
Re_eq=Re_v*(mu_v/mu_l)*(rho_l/rho_v)^.5+Re_l;       "equivalent reynold number"
Pr_l=mu_l*c_p_l/K_l ;                               "prandlt number"
h_i=.05*Re_eq^.8*Pr_l^.33*k_l/d_t_i;                "internal heat transfer coeff"

"calculation of heat transfer by using variable conductance approach"
R_i=1/(h_i*pi*d_t_i*z);                             "inner resistance"
R_t=ln(d_t_o/d_t_i)/(2*pi*k_f*z);                   "tube resistance"
R_ele=R_i+R_t+R_o_eq;                               "elemental resistance"
UA_ele=1/R_ele;                                     "conductance"
U= UA_ele/ A_b_p                                    "overall heat transfer coeefficient"
Q_dot_ele=U*A_b_p*(T_ref-T_infinity);               "heat rejected"

"calculation for outer tube temperature"
T_t_o=T_ref-Q_dot_ele*(R_i+R_t);

"enthalpy of the refrigerant at the outlet"
E_h_0=h_ref-Q_dot_ele*convert(W,kW)/m_dot;

"pressure drop calculation"
"frictional pressure drop"
m_dot_l=m_dot*(1-x);                                "liquid mass flow"
m_dot_v=m_dot*x;                                    "vapour mass flow"
x_tt=(m_dot_l/m_dot_v)*sqrt(rho_v/rho_l)            "Martinalli parameter"
phi_l=sqrt(1+8/x_tt+1/x_tt^2);                      "correction factor"
f_l=(.79*ln(Re_l)-1.64)^(-2);                       "fricton factor"
dpdz_l=f_l/d_t_i*m_dot^2/2/rho_l/L^4
dpdz_f=phi_l^2*dpdz_l;                              "frictional pressure drop per unit length"
deltap_f=dpdz_f*l_t_b                               "frictional pressure drop"

"pressure drop due to acceleration"
rho_0=Density(R134a,T=T_t_o,h=E_h_0)                "density at outlet"
deltaP_a=G^2*(1/rho_i-1/rho_0)                      "pressure drop due to acceleration"

"gravitational pressure drop"
gaama=.99                                           "void fraction"
dpdz_g=(gaama*rho_v+(1-gaama)*rho_l)*g#
deltap_g=dpdz_g*l_t_b                               "pressure drop due to gravity"

"total pressure drop"
deltap*convert(kPa,Pa)= deltaP_a+ deltap_f +deltap_g    "total pressure drop"
```

"pressure at outlet"
p_outlet=P_ref-deltap **"pressure at outlet"**

"condition at output of back panel "
T_2=T_t_o; **“temperature at outlet”**
p_2=p_outlet; **“pressure at outlet”**
rho_2 = rho_0; **“density at outlet”**
E_h_2=E_h_0; **“enthalpy at outlet”**
x_2=Quality(R134a,T=T_2,h=E_h_2); **“dryness fracttion at outlet”**

SOLUTION
Unit Settings: [kJ]/[K]/[kPa]/[kg]/[degrees]

α_a = 0.00002244 [m2/s]
A_c = 0.00001256 [m2]
β_a = 0.003273 [1/K]
$cp_{,l}$ = 1497 [J/kg-k]
δp = 11608[kPa]
δp_f = 110959 [kg/m-s2]
dpdzf = 11510 [kg/m2-s2]
dpdzl = 0.0502 [kg/m2-s2]
$d_{t,o}$ = 0.00475 [m]
ηplate = 0.9962
$E_{h,2}$ = 304.18[kJ/kg]
G = 79.58 [kg/s-m2]
z = 8.93 [m]
h = 7.892 [w/m2-K]
$h_{b,p}$ = 1.4 [m]
hi = 2074 [w/m2-K]
h_{ref} = 417.73 [kJ/kg]
k_f = 15.47 [w/m-K]
k_v = 0.0154 [W/m-K]
L_{cha} = 1.4 [m]
m = 2.373 [m(-1)]
μ_l = 0.000161 [kg/m-s]
m = 0.001 [kg/sec]
m_v = 0.00099 [kg/sec]
φ_l = 478.8
Prl = 3.226
p_{outlet} = 895.7 [kPa]
Q_2 = 100.2 [W]
Ra = 3.504E+09
Re_l = 19.77
ρ_0 = 150.72 [kg/m3]
ρ_a = 1.156 [kg/m3]

$A_{b,p}$ = 0.8736 [m2]
A_i = 0.00001257 [m2]
cp_a = 1005 [J/kg-K]
$cp_{,v}$ = 1143 [J/kg-k]
δP_a = 83.72 [kg/m-s2]
δp_g = 5752 [kg/m-s2]
dpdzg = 596.7 [kg/m2-s2]
$d_{t,i}$ = 0.004 [m]
epcilen = 0.859
$E_{h,0}$ = 304.18 [kJ/kg]
f_l = 1.942
gaama = 0.99
x_{tt} = 0.002106
h_0 = 7.892 [w/m2-K]
h_c = 2.347 [w/m2-K]
h_r = 5.545 [W/m2-K]
k_a = 0.02606 [W/m-K]
k_l = 0.0747 [W/m-K]
L = 0.04531 [m]
$lt_{,b}$ = 9.64 [m]
μ_a = 0.00001883 [kg/m-s]
μ_v = 0.0000123 [kg/m-s]
m_l = 0.00001 [kg/sec]
Nus = 126.1
Pra = 0.7263
p_2 = 895.7 [kPa]
p_{ref} = 1012.5 [kPa]
Q_{ele} = 100.2 [W]
Re_{eq} = 9408
Re_v = 25620
ρ_2 = 150.72 [kg/m3]
ρ_i = 50.35 [kg/m3]

ρ_l = 1147 [kg/m3]
R_{ele} = 0.1498 [k/w]
$R_{o,eq}$ = 0.1456 [k/w]
R_t = 0.0001834 [k/w]
T_2 = 312.6 [k]
T_{av} = 312.8 [k]
$T_{pl,av}$ = 312.5 [K]
Tt,o = 312.6 [k]
UA_{ele} = 6.868 [w/k]
x = 0.999

ρ_v = 49.87 [kg/m3]
R_i = 0.003979 [k/w]
R_{pl} = 0.2912 [k/w]
T_0 = 312.6 [k]
T_a = 305.5 [K]
T_∞ = 298 [k]
T_{ref} = 313 [k]
U = 7.862 [w/m2-K]
$w_{av,b}$ = 0.09062 [m]
x_2 = 0.297